Progress in NMR Spectroscopy, 1978, Vol. 12, pp. 41–77. Pergamon Press. Printed in Great Britain

THE NMR RECEIVER: A DESCRIPTION AND ANALYSIS OF DESIGN

D. I. HOULT
Department of Biochemistry, University of Oxford, South Parks Road, Oxford, England

(*Manuscript Received* 14 *April* 1977)

CONTENTS

1. INTRODUCTION

The performance of a nuclear magnetic resonance (NMR) spectrometer, in terms of sensitivity and faithfulness of reproduction of spectral information, is determined to a very large extent by the design of what is loosely termed the "receiver" and, in many cases of non-routine operation, by the spectrometer operator's understanding of how the receiver works, its limitations and its peculiar characteristics. The design of a good receiver is a considerable exercise in electronic engineering, and the aim of this article is therefore firstly in Sections 2–7, to explain in simple terms the working of an NMR receiver and secondly in Sections 8–12, to analyse in greater detail the criteria affecting the design of each stage. Now of course the exact minutae of circuitry and layout vary from one manufacturer to another, but as the author is not intimately familiar with any commercial machine, preferring to build his own, he cannot but help irritate most readers by not describing exactly their instrument. However, the reverse of this particular coin is that he cannot be accused of bias! In the belief however that most electronic engineers have converged

on similar solutions to the same problems, it is hoped that the following pages will be an aid to those users wishing to improve their understanding of their instrument.

2. THE RECEIVER—A DEFINITION

Information concerning the particular substance of interest in an NMR experiment is locked away in the interaction of the nuclei with one another, with the lattice and of course with the externally applied magnetic field B_0, and to extract the information, it is necessary to perturb the system in an intelligent manner. By way of analogy, a piano is tuned in a particular way, and that information is locked away inside the instrument. To extract it, we have to hit the keys of the piano so perturbing the "system"—in this case, the various strings under tension and hence in a resonant condition. Now the information obtained is directly assimilable to the trained ear. We recognise definite frequency intervals and varying amplitudes without the need for any electronics; the results stimulate a human sense directly. Unfortunately, however, we have no senses for detecting a precessing nuclear magnetic moment, and it is of course, the latter which is obtained when the resonant condition of the nuclear system is exploited by means of a perturbation, applied B_1 transverse irradiation. The receiver therefore is the interface, between the NMR system and a human being, which converts the results of the perturbation into a form which "makes sense"; normally visual sense but exceptionally, aural sense. Under this definition, the receiver may include a computer, though this will be dependent upon the manner in which the system is perturbed. To return to our piano analogy, if the notes are played sequentially and slowly, we hear a clear progression of frequency, but if all notes are played simultaneously we shall surely need a computer to analyse all the different frequencies present. To summarise then, the requirements of the receiver will be dependent upon

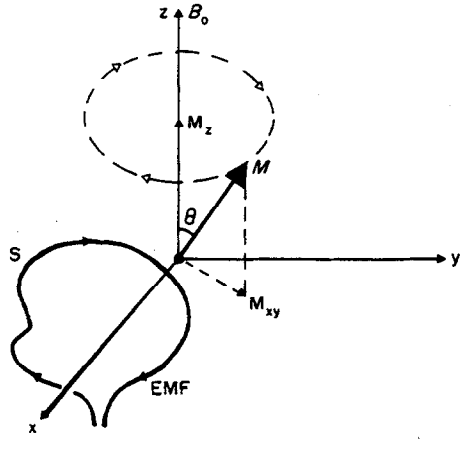

FIG. 1. The rotating magnetisation M induces an EMF in the coil S.

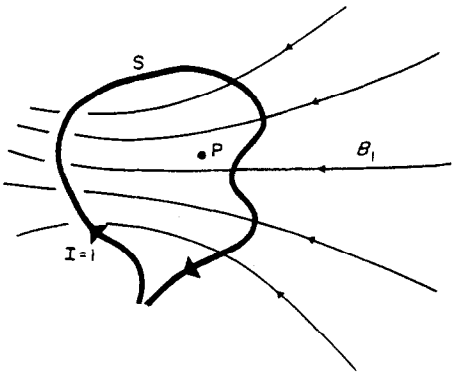

FIG. 2. The signal from point P is proportional to the B_1 field at that point.

the manner in which the system is perturbed, but in general, the greater the flow of information through the receiver, the more sophisticated it will need to be in order to present results that we can "take in".

Ideally, the receiver should not throw away any of the information available. Unfortunately, the Laws of Thermodynamics have something to say on this subject, and it is well known that NMR is an insensitive technique. However other information is also sacrificed, mostly for technical reasons which involve compromises of cost, sensitivity etc. How many spectrometers for example give information as to the sign of the nuclear magnetogyric ratio, γ? Yet this information is always present. Let us therefore consider the various ways in which the presence of a precessing nuclear magnetic moment may be detected and what steps we must take to present the available information to the best of our ability.

3. THE PROBE

3.1. *The Signal*

There are various methods of detecting the occurrence of a magnetic resonance condition. The most obvious involve monitoring the change in bulk magnetic susceptibility by means of a sensitive balance[1] or a Josephson junction[2] or even by neutron scattering.[3] However, the most sensitive method to date relies on the principle of induction, i.e. a changing magnetic field induces an electromotive force (EMF) in a loop of electrical conductor through which the field passes. Now the details concerning the manner in which an NMR system is driven or perturbed lie mostly outside the scope of this article. Fuller accounts may be found in references (4) and (5); suffice it to say for the moment that the effect of the perturbation is usually to produce a bulk component of magnetisation M per unit volume which precesses about the main field B_0 with an angular velocity given by

$$\omega_0 = -\gamma B_0 \qquad (1)$$

M may or may not be time dependent, depending upon the method of perturbation. Consider therefore

the situation shown in Fig. 1 where the rotating magnetisation M produces an alternating magnetic field at the loop of conductor S. By intuition, we can say that if M is close to the loop a large EMF will be induced, whereas if M is far away, the EMF induced will be small. This statement can be quantified in the following way. Suppose unit current is passed through the loop of wire S. A magnetic field B_1 will be created which is large close to the loop and small far away from it. This is shown in Fig. 2. There is a direct correspondence between the EMF induced in loop S by an elementary rotating magnetic moment $M\delta V_s$ at point P, and the magnetic field B_1 at point P produced by unit current flowing in the loop. Using this Principle of Reciprocity,[6] it may be shown that the EMF induced in the loop is given by

$$\delta\xi = -\frac{\partial}{\partial t}\{B_1 \cdot M\}\,\delta V_s \tag{2}$$

where δV_s is an elementary sample volume. Now M is given by

$$M = M_{xy}\,e^{j(\omega_0 t+\sigma)} + M_z \tag{3}$$

where the time dependence of the amplitude of M has been ignored, and

$$M_{xy} = M\sin\theta, M_z = M\cos\theta, j = \sqrt{-1}. \tag{4}$$

The phase of the magnetisation, σ, is dependent upon the driving irradiation, and may therefore be a function of spatial position P. It follows that the EMF induced in the coil by the moment at point P is given by

$$\delta\xi = -\frac{\partial}{\partial t}\{[B_{1xy}e^{j\phi} + B_{1z}]\cdot[M_{xy}e^{j(\omega_0 t+\sigma)} + M_z]\}\,\delta V_s$$

where B_1 has been expressed as the sum of components perpendicular and parallel to B_0—i.e. the z axis. When this expression is evaluated, we find that

$$\delta\xi = \omega_0 B_{1xy} M_{xy}\sin(\omega_0 t + \sigma - \phi)\delta V_s \tag{5}$$

and so the signal from the entire sample can be evaluated by integrating this expression over the sample, noting that B_{1xy}, M_{xy}, σ and ϕ will, in general, be functions of position.

There are several points to note about eqn (5). Firstly, the magnetisation M is derived, by the perturbation from the static equilibrium magnetisation M_0 which is given by

$$M_0 = \frac{N\gamma^2\hbar^2 I(I+1)B_0}{3kT_s} \tag{6}$$

where N is the number of spins at resonance per unit volume, I is the spin quantum number and T_s is the sample temperature. As $\omega_0 = -\gamma B_0$ it follows from eqn (5) that as M is proportional to ω_0, the induced EMF is proportional to ω_0^2. Secondly, B_{1xy} can in principle be calculated for any loop of conductor with unit current flowing through it and so we have a means of evaluating, for any given coil configuration, the amplitude of the EMF induced by a perturbed volume of sample. This calculation is typically performed when the entire sample has been perturbed by a 90° pulse, in which case M_{xy} is known accurately and is equal to M_0. Thirdly, σ, the phase of the precessing magnetisation is not usually known relative to the laboratory frame of reference and so eqn (5) gives no information as to whether γ, the magnetogyric ratio, is positive or negative. Consider however the situation if we have *two* receiving coils, each of which, when carrying unit current, produces a field B_{1xy} *in amplitude*, but which are orthogonal to each other.[7] Then from the first we have from eqn (5) that

$$\delta\xi_A = \omega_0 B_{1xy} M_{xy}\sin(\omega_0 t + \sigma - \phi)\delta V_s$$

whereas for the second,

$$\delta\xi_B = \omega_0 B_{1xy} M_{xy}\sin(\omega_0 t + \sigma - \phi + 90°)\delta V_s$$
$$= \omega_0 B_{1xy} M_{xy}\cos(\omega_0 t + \sigma - \phi)\delta V_s.$$

Written in complex form we have that

$$\delta\xi = \delta\xi_B + j\delta\xi_A =$$
$$\omega_0 B_{1xy} M_{xy}\exp j(\omega_0 t + \sigma - \phi)\delta V_s. \tag{7}$$

In the complex plane (which if a high frequency oscilloscope were available might be displayed by letting the x deflection be ξ_B and the y deflection be ξ_A) the direction of rotation is clearly dependent on ω_0 and hence upon the sign of γ. In principle then, by having two receiving coils "in quadrature" the sign of the magnetogyric ratio may be determined. In practice, except at low frequencies (<10 MHz) the experiment is difficult to perform as the two receiving coils and their associated circuitry interact and true electrical orthogonality is difficult to attain.

It is quite clear from eqn (5) that to obtain the maximum signal, the magnetic field B_1 associated with unit current in the receiving coils should be predominantly in the xy plane so that B_{1xy} is maximised. Also, when eqn (5) is integrated it becomes apparent that the phase ϕ of B_{1xy} should not vary significantly over the sample volume as this too can reduce the signal obtained. This statement is true only for crossed-coil systems. However as shown in Section 9.2, the presence of B_1 inhomogeneity can give rise to spinning sidebands as well as causing errors in relaxation time measurements.[8]

When designing receiving coils one therefore aims to produce a coil system which has a homogeneous B_1 field which is predominantly in the xy plane. The manner in which this is accomplished is dependent upon the magnet system employed. With a conventional iron magnet as shown in Fig. 3, the coil is most conveniently a solenoid into which sample tubes can be slid. However if a superconducting magnet is employed, the situation is complicated by the fact that the axis of the sample is usually parallel to the main field B_0 as shown in Fig. 4. The main cause of this situation is that superconducting magnets are

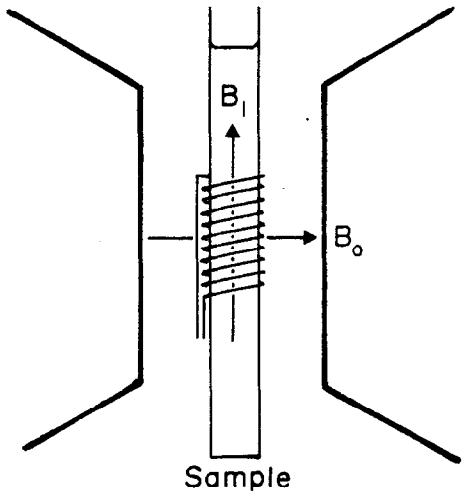

FIG. 3. The sample and coil configuration used with an iron magnet.

conventionally wound in solenoidal form and the bore through the centre is too narrow to permit the use of a transverse sample. Hence to produce a transverse field B_1, saddle-shaped or Helmholtz receiving coils are needed. For both solenoidal and saddle-shaped coils (which are discussed in more detail in Section 8.1) the B_1 field produced by unit current can be calculated and for similar dimensions both coil configurations give similar fields and hence receive about the same induced EMFs. As will be seen below, however, this does not mean that the two types of receiving coil are equally efficient.

3.2. *The Noise*[9]

So far, we have seen that the signal induced in a receiving coil by a precessing nuclear magnetic moment can be calculated if the B_1 field produced by the coil at the magnetic moment is known. Typically, the induced EMF is in the range of 10^{-9}–10^{-5} volts and unfortunately this range includes the EMF values associated with Brownian motion of electrons in an electrical conductor. The phenomenon of resistance in a conductor is a manifestation of the interaction between electrons and the lattice, and if electrical energy in the form of motion of the electrons (a current) is available then the interaction converts the electrical energy into thermal energy and the conductor becomes hot. Only at very low temperatures, for certain conductors, does the interaction cease. Conversely, the interaction can convert thermal energy into electrical energy, and this may be detected as random fluctuations of EMF across the two ends of a conductor. From the above it is clear that the size of these random fluctuations is dependent upon the strength of the interactions (of which the electrical resistance is a measure) and the rate at which interactions take place (of which temperature is a measure). Only in the case of zero resistance and/or zero temperature are there no thermal EMFs generated in a conductor. Now any such function which varies with time can be considered, via the mechanism of Fourier analysis, to comprise a sum of sinusoids of appropriate amplitudes, phases and frequencies, and in a NMR experiment we are interested in detecting a small range of Larmor frequencies (say 10 kHz) at a frequency of many MHz. We must therefore consider how the thermal EMF values (or noise) vary with frequency, and in particular, what their values are about the Larmor frequency of interest. There arise now some conceptual difficulties which, as they occur whenever Fourier analysis is invoked (e.g. in pulsed Fourier experiments), are worth considering in some detail. They centre around the question of defining frequency. In general, we can only observe a given situation for a finite length of time and so, if we are measuring say the frequency of an oscillating function, we can only perform the measurement to a certain degree of accuracy. Obviously the longer we measure, the greater the accuracy of the result. The Uncertainty Principle states that the appropriate relationship between the two conjugate variables, frequency and time, is

$$\Delta\nu\,\Delta t \sim 1 \tag{8}$$

and thus in an observation lasting a time Δt, our frequency resolution is no better than $\Delta\nu \sim 1/\Delta t$. Hence, if we attempt to measure the component at a given frequency (of say noise) we will fail. We will measure the sum total of the noise over a band of frequency $\Delta\nu$ centred on the frequency of interest. Although we are concerned here with noise, this principle is clearly valid for any situation where Fourier's theorem is invoked and an understanding of its application is of vital importance.[10]

Thermal EMF, or noise, is therefore defined as an *incremental* function, and the mean thermal power available in electrical form is given by

$$dP/d\nu = 4kT \tag{9}$$

where P is power measured in watts, k is Boltzmann's constant and T is absolute temperature. As has been stated, this energy is associated with resistance r, and

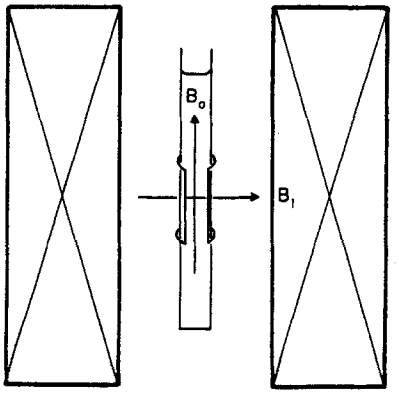

FIG. 4. The sample and coil configuration used with a superconducting solenoid.

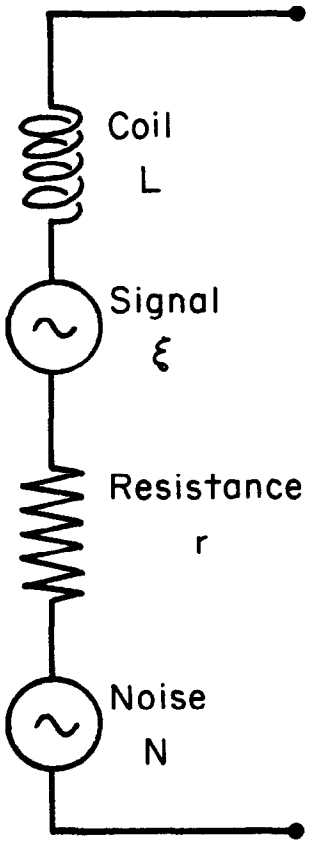

FIG. 5. The equivalent circuit of the probe coil.

the instantaneous power available is given by N^2/r where N is the instantaneous noise voltage. Hence the mean power between frequencies $\nu - \Delta\nu/2$ and $\nu + \Delta\nu/2$ is given by

$$\frac{\overline{N^2}}{r} = \int_{\nu-(\Delta\nu/2)}^{\nu+(\Delta\nu/2)} 4kT\,d\nu = 4kT\,\Delta\nu$$

which, it should be noted, is independent of the frequency. Thus the root mean square noise EMF over a bandwidth $\Delta\nu$ at the Larmor frequency of interest is given by

$$N_{RMS} = (\overline{N^2})^{1/2} = \sqrt{4kTr\,\Delta\nu}. \qquad (10)$$

From this equation we can calculate the noise associated with the probe receiving coil and thus, with the aid of eqn (5) which gives the signal, calculate the signal-to-noise ratio of the probe. If the spectrometer is well designed, this ratio should be that given by the entire instrument, but needless to say, there are many ways in which the ratio can be degraded between the probe and the final spectrum. Sections 8 and 9 deal with the factors which influence the design of good receiving coils in more detail, but it is obvious that to get the most signal, B_1 must be maximised, and to obtain the least noise r must be minimised. The coil resistance (typically $\sim 0.5\,\Omega$) is very dependent upon the manner in which the coil is wound, and the resistance of, for example, a saddle-shaped coil may well be four to ten times greater than that of a solenoidal receiving coil. The sensitivity of a saddle-shaped probe is therefore correspondingly less (by a factor of two to three) which accounts to some extent for the slightly disappointing performance of superconducting magnet spectrometers.

Our results so far may therefore be summarised in Fig. 5, where the coil (of inductance L) and its resistance r are shown, together with EMFs for the signal and noise respectively. Let us now pursue the subject of noise a little further as it will be of subsequent interest. Many difficulties will be avoided if it is remembered that noise is primarily a manifestation of thermal energy. Thus it is associated *only* with resistance. Inductance and capacitance, being energy *storage* mechanisms, generate of themselves no noise. Of course if a source of thermal noise *is* present, inductive and capacitive elements in a circuit can alter the EMF and change the phase of noise in a particular frequency band, but they can never add to or subtract from the thermal *energy* available—energy is conserved by them. Thus if a particular reactive* circuit increases the thermal EMF of some resistive source, then the effective resistance of that source must increase correspondingly so that the power $\overline{N^2}/r$ is conserved. A particularly simple and familiar example of this effect is a transformer. If it doubles the EMF of a source of resistance r, it is well known that the new effective source resistance is $4r$. This is shown in Fig. 6, and further examples, involving tuned circuits, will be considered later.

Now we have talked about noise in a particular frequency band, so let us consider what happens when we attempt a Fourier analysis of thermal EMF. Figure 7 shows the first twenty points in a Fourier transform of noise which was observed for Δt seconds. Clearly, the phase is a totally random function of frequency, but the amplitude is not, having the average value shown. Thus it is often useful when analysing how a circuit affects noise, to assume that in each bandwidth $\Delta\nu = 1/\Delta t$, the noise EMF has a value given by $\sqrt{4kTr\Delta\nu}$, but the phase is random. Let us assume now a "black box" circuit which has a normalised (passive) transfer function $G(\nu)$, in other words, output = $G(\nu)$ times input, and let us assume that the output is connected, as shown in Fig. 8, to a very

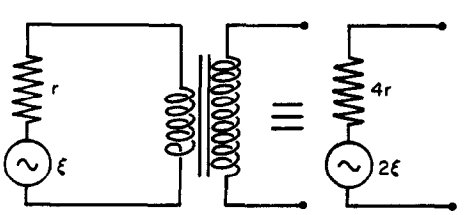

FIG. 6. A transformer conserves the available source energy.

* Reactive implies inductive and/or capacitive.

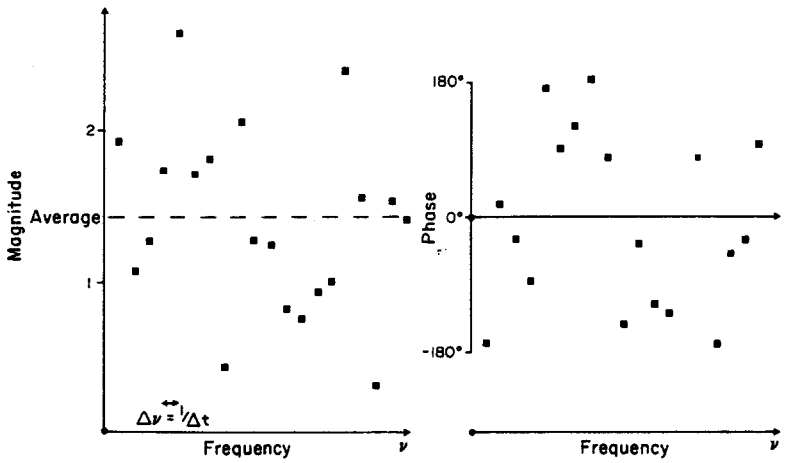

FIG. 7. The frequency spectrum of noise.

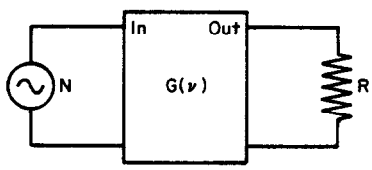

FIG. 8. "Black box" transfer function.

large resistance R. Then the power dissipated in R at frequency ν is given by

$$P = \overline{N^2}/R = (4kTr\Delta\nu/R)\, G(\nu)G(\nu)^*,$$

in bandwidth $\Delta\nu$. Summing over all frequencies we have that in the limit as $\Delta\nu \to 0$,

$$P = \int_0^\infty 4kT\frac{r}{R}G(\nu)G(\nu)^*\,d\nu.$$

The voltage developed across the resistance R is thus given by

$$N_{RMS} = \sqrt{4kTr}\sqrt{\int_0^\infty G(\nu)G(\nu)^*\,d\nu}$$

and the noise equivalent bandwidth of the circuit is thus

$$\Delta\nu' = \int_0^\infty G(\nu)G(\nu)^*\,d\nu. \qquad (11)$$

The important point to note is that because the phase of each frequency component is random, the total root mean square (RMS) noise obtained when components at different frequencies are summed is dependent on the *square root* of the number of points summed. We can use the same type of analysis to show that if thermal noise is integrated, the RMS value after a time t is proportional to $\sqrt{t}$. The process of integration is similar to applying a transfer function with a gain of t and an equivalent bandwidth of $\Delta\nu = 1/2t$. Similarly, if equal noises from two sources are summed, the resultant is only $\sqrt{2}$ greater than the noise from a single source. *Noise powers add.*

* Impedance is resistance and reactance.

4. THE PRE-AMPLIFIER

4.1. *The Noise Figure*

The signal and noise obtained from the probe receiving coil may be considered to have very delicate health and our first aim must be to amplify them without injuring them (i.e. without distortion or the addition of extra noise). The aim of this process is to allow us to be careless about noise later on in the receiver, for when the signal is more robust, it is treated to rather noisy indignities such as phase sensitive detection. However, for the moment, let us consider a high frequency pre-amplifier which is represented, for simplicity, in Fig. 9 as a black box, with gain A, which introduces some extra noise whose RMS value is N_A. Further let there be attached to the amplifier a signal source with source impedance* $Z = R + jX$, and corresponding noise $N_S = \sqrt{4kTR\Delta\nu}$. The bandwidth, $\Delta\nu$, is assumed to be limited by the equipment that we use to measure the output and so affects N_A as well as N_S. The total noise output of the pre-amplifier is $A(N_A^2 + N_S^2)^{-1/2}$ (remembering that it is noise powers which add) whilst the signal output is ξA. The output signal-to-noise ratio is thus $\xi(N_A^2 + N_S^2)^{-1/2}$. Now if the amplifier were perfect, the ratio would be ξ/N_S, and so a measure of the quality of the pre-amplifier is the ratio of these two quantities, i.e. $(N_A^2 + N_S^2)^{1/2}/N_S$

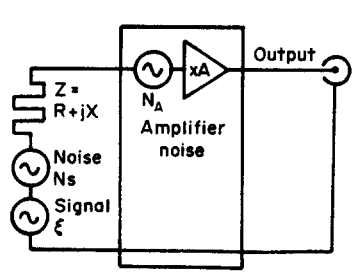

FIG. 9. An idealised pre-amplifier. It is followed by measuring equipment with bandwidth $\Delta\nu$.

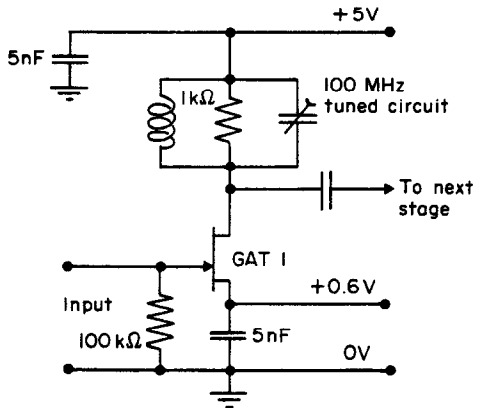

FIG. 10. The basic circuit of a pre-amplifier. The load is tuned to the frequency of interest.

and in practice, this is usually expressed in decibels and called the noise figure F.

$$F = 10\log_{10}\left\{\frac{N_A^2 + N_S^2}{N_S^2}\right\} \qquad (12)$$

A poor pre-amplifier has a noise figure greater than three decibels, in which case the signal-to-noise ratio is degraded by a factor of greater than $\sqrt{2}$, whilst a good pre-amplifier has a noise figure of less than 1 dB, corresponding to a degradation of less than 12%. Strictly speaking, eqn (12) is defined for a source at a temperature of 290 K; in practice this is room temperature.

Now suppose with the aid of, for example, a transformer we increase (prior to the pre-amplifier) the signal ξ by a factor B. Then the effective source resistance is no longer R but B^2R, as has been discussed earlier, and the noise, EMF, N_S, is also increased by a factor B. It would appear from eqn (12) that as $B \rightarrow \infty$, $N_S \rightarrow \infty$ also, and so the noise figure F tends to zero (a perfect pre-amplifier). Unfortunately, this is not the case, for it transpires that for any amplifier, N_A depends on Z in a complicated way which is a function of the manner in which the pre-amplifier is constructed, and also of frequency.[11] Thus at any particular frequency, there is an optimum value of source impedance Z which yields the best noise figure. A prevalent mistake is the assumption that Z should equal the input impedance Z_{in} of the pre-amplifier (which is not shown in Fig. 9). A little thought shows that this cannot be the case as the noise figure would be worse than 3 dB, the input resistance R_{in} contributing as much noise as the source. The input impedance of the pre-amplifier must be very much *greater* than Z, so that the noise associated with R_{in} is effectively short circuited by Z.

4.2. *Noise Matching the Probe*

Let us now consider a practical case. Figure 10 shows the input circuit of a gallium arsenide field effect transistor (FET) pre-amplifier designed to work at about 100 MHz. This particular device has a noise figure at room temperature and 100 MHz of about 0.5 dB when working from a source impedance of about 800 Ω resistive ($jX \simeq 0$). (A description of the working of FETs may be found in many standard texts on electronics, e.g. reference 12.) Now our probe is, electronically speaking, the circuit of Fig. 5 which typically, might comprise a resistance r of about 0.5 Ω and an inductive reactance of about j 100 Ω. We must therefore transform this impedance in a lossless manner (i.e. without introducing any further resistance and hence noise) to the required 800 Ω resistive. It must be said immediately that a transformer is useless for this purpose and in general, at frequencies greater than 1 MHz, the use of transformers should be avoided in low-noise applications as they introduce losses. The quality factor Q is a measure of the efficiency of reactive devices and in general, inductors have Q values less than 300. On the other hand, first class capacitors can have Q values in excess of 3000. The quality factor at any frequency is given by

$$Q = \frac{X}{r} = \frac{2\pi\nu L}{r} \qquad \text{for an inductor}$$
$$= \frac{1}{2\pi\nu rC} \qquad \text{for a capacitor} \qquad (13)$$

and we may see that with the typical values chosen, the probe has a Q of 200. Let us therefore consider the ways in which high Q capacitors may be used to transform the impedance of the probe coil to the required value. If a capacitor is connected across the coil, as shown in Fig. 11 a resonant circuit is produced. That this is so may be confirmed experimentally with the circuit of Fig. 12 where the ringing pattern of the resonant circuit is observed with the aid of a high-frequency oscilloscope. Below about 100 MHz, this circuit also allows one to measure the Q of the circuit, for the ringing pattern which occurs when the current through the diode is rapidly turned off is given by

$$V = e^{-t/\tau}\cos 2\pi\nu_0 t \qquad (14)$$

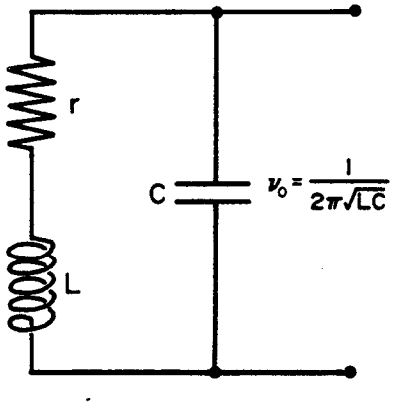

FIG. 11. A resonant circuit. The inductive reactance $j2\pi\nu_0 L$ cancels the capacitive reactance $(j2\pi\nu_0 C)^{-1}$, and hence the resonant frequency $\nu_0 = 1/[2\pi(LC)^{1/2}]$.

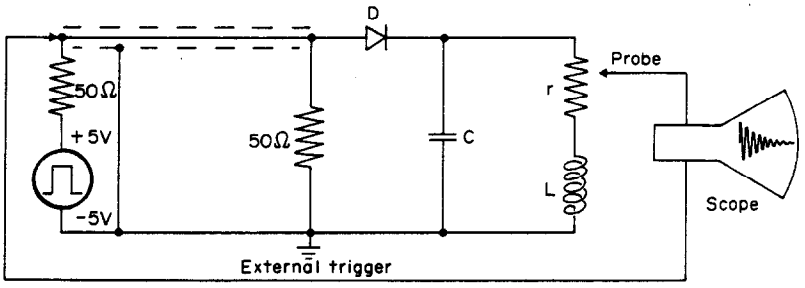

FIG. 12. The ringing of a tuned circuit. The fall time of the pulse should be <20 ns, and the diode should have a reverse recovery time of 2 ns or less with a capacitance, when reversed biassed, of $\ll C$. These conditions limit the usefulness of the circuit to less than about 100 MHz. The oscilloscope probe should not touch the circuit as it will dampen the ringing. The Q of the circuit is given by $Q = \pi\tau\nu_0$, where τ is the time constant of the decay and ν_0 is the frequency.

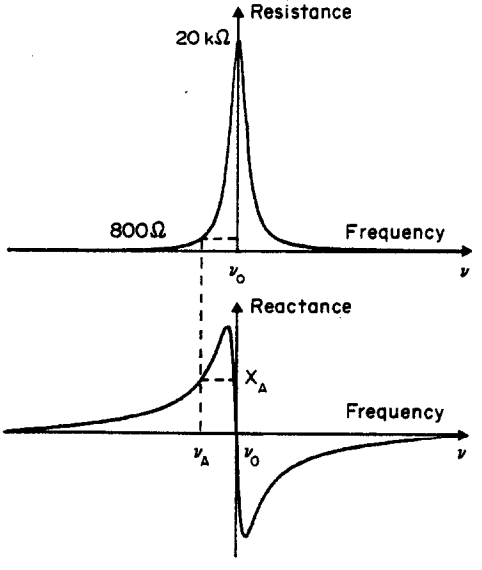

FIG. 13. The impedance of a tuned circuit.

where $\tau = Q/\pi\nu_0 = 2L/r$, if the resistance of the capacitor can be neglected. Now the ringing pattern of eqn (14) is well known in NMR spectroscopy—it is a free induction decay, and the Fourier transform is of course a Lorentzian line. In this context, the absorption mode, or real part, is the resistance of the tuned circuit of Fig. 11 whilst the dispersive, or imaginary, part is the reactance. This is shown in Fig. 12 and on resonance, the peak height is $Q2\pi\nu_0 L$ Ω, which in our case is about 20 kΩ. Now consider the situation at frequency ν_A. The impedance of the circuit at this frequency is given by $Z = 800 + jX_A$ which is effectively a resistance of 800 Ω in series with an inductance whose reactance is jX_A. However this reactance can be cancelled by the addition of a capacitor C' whose reactance $(j2\pi\nu_A C')^{-1}$ is $-jX_A$. Thus the circuit of Fig. 14 allows one, simply by the use of low loss capacitors, to transform from $Z = 0.5 + j\,100\,\Omega$ to 800 Ω resistive without the introduction of extra noise. Capacitor C', whose value is given by

$$C' \simeq \sqrt{\frac{C}{QY2\pi\nu_A}}; \qquad C' \ll C, \tag{15}$$

where Y is the resistance value required (in this case 800 Ω), effectively determines the size of the transformation, whilst capacitor C determines the frequency at which it takes place, assuming of course one has approximately correct values to start with. A variant on this circuit is shown in Fig. 15.

Here $$C' \simeq \sqrt{\frac{CQ}{2\pi\nu_A Y}}; \qquad C' \gg C, \tag{16}$$

and C' and C fulfil the same functions as before. Needless to say, whenever the Q of either circuit is measured, it should be disconnected from any cables and from the pre-amplifier to avoid false readings. Having obtained, with the aid of the circuit of Fig. 12, the approximately correct value of C for the frequency of interest, it is worth noting that the correct value of C' may be obtained by adding to the resonant circuit C' in series with (for Fig. 15, in parallel with) the desired resistance value, 800 Ω. The value of C' is correct when it halves the measured Q value.

Figure 16 shows the circuitry of a typical receiving coil and pre-amplifier of the "cascode" type, which utilises two MOSFETS to obtain a noise figure of about 2 dB. The second transistor helps to isolate

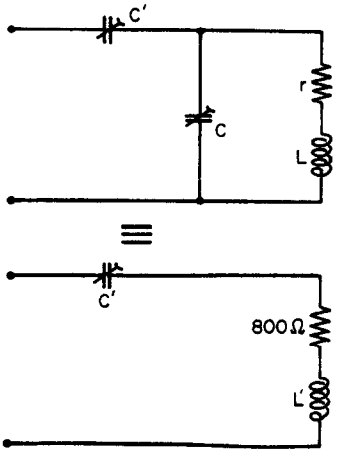

FIG. 14. The probe matching circuit.

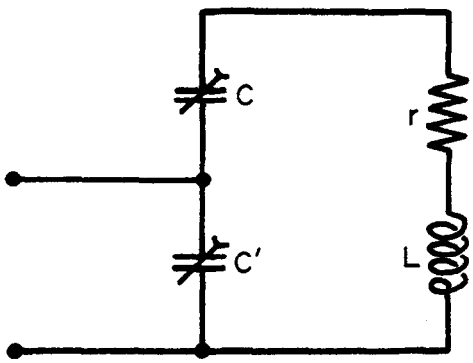

FIG. 15. Another method of probe matching.

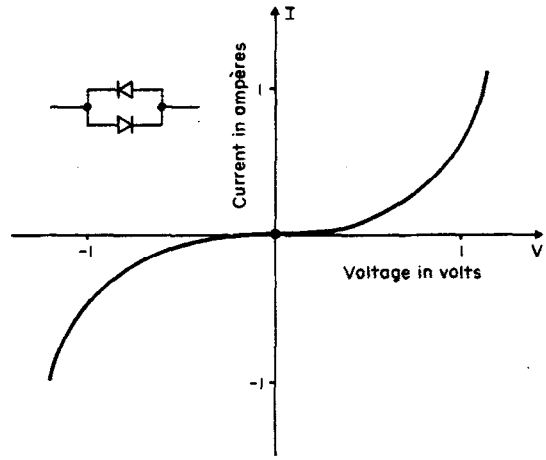

FIG. 17. "Crossed diodes". Their approximate characteristics.

the amplified signal from the input and hence improves the stability of the pre-amplifier.

4.3. *Single Coil Configurations*

So far, we have concerned ourselves only with the received signal. However we must not overlook the fact that whilst the transmitter which drives the nuclear resonances is on, there may occur voltages at the pre-amplifier which can destroy the transistor connected to the receiving coil. This problem is at its most acute in Fourier transform, cross-polarization and other pulse experiments where powers up to 10^3 W are commonly used for short periods of time, and the pre-amplifier must therefore be protected in some manner. The most prevalent method of protection involves the use of "crossed diodes" as shown in Fig. 17. When small voltages ($\ll 1$ V) are present the diodes do not conduct and their presence may be ignored. On the other hand, when large powers are used, the diodes conduct and present, on average, a very small impedance. Needless to say, the correct diodes, in terms of power dissipation and cut-off frequency, must be chosen for the particular situation, and it must be remembered that when "off" the diodes will have a capacitance of a few picofarads and when "on" an inductance of a few nanohenries.

If large powers are used with a crossed-coil probe (i.e. the transmitter and receiving coils are separate and orthogonal) then, in Fig. 16 crossed diodes may be placed across capacitor C' to protect the FET. However, if the same coil is used for transmission and reception, major changes in probe and pre-amplifier design may be needed. The reason for this lies in the way high frequency electrical power is carried over distances greater than a fraction of a wavelength.[13] In such a case, there is always the possibility of power being lost "through air", by electromagnetic radiation, and so a shield must be placed about the conductor to prevent this. Radio frequency (RF) power is therefore carried in coaxial cable, as shown in Fig. 18. Such cable obviously has inductance and capacitance per unit length which is dependent on the dimensions of the conductor and the dielectric constant of the insulator. In turn, the velocity of the radiation down the cable is also determined by the dielectric constant, and for polyethylene dielectric, which is commonly employed, the velocity of propagation is 2.0×10^8 ms^{-1}. Associated with the inductance and capacitance is an impedance, i.e. by Ohm's law there is a definite relationship between the voltage

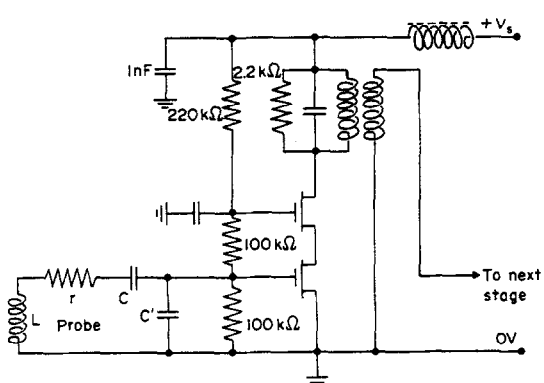

FIG. 16. A probe and pre-amplifier for a continuous wave spectrometer. The component values depend upon the transistors and the frequency.

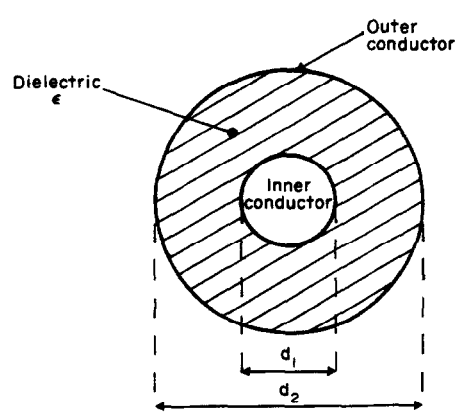

FIG. 18. Co-axial cable.

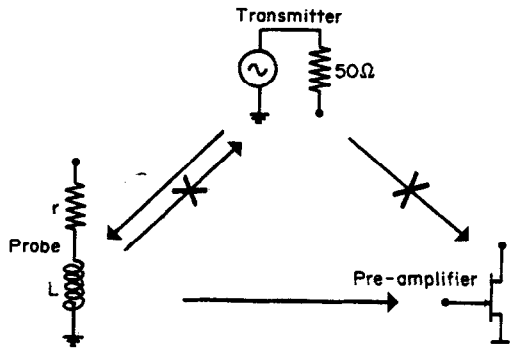

FIG. 19. The matching problem.

and current in a co-axial conductor, and typically the characteristic impedance is 50 Ω, though 75 Ω and 200 Ω cables are also used. The impedance, referring to Fig. 18, is given by

$$Z_0 = \frac{1}{2\pi}\sqrt{\frac{\mu\mu_0}{\epsilon\epsilon_0}}\log_e\left(\frac{d_2}{d_1}\right). \tag{17}$$

Once the length of such cable is greater than a fraction of a wavelength, the electrical power transmitted down it may be thought of as a wave motion and if none of this wave is to be reflected at the end of the cable, the latter *must* be terminated with a *resistance* of Z_0. If it is not, the reflection coefficient is given by

$$\rho = Z - Z_0/Z + Z_0 \tag{18}$$

where Z is the terminating impedance.

Thus termination in a short circuit ($Z = 0$) reflects all the power, but with a 180° change of phase ($\rho = -1$); termination in an open circuit ($Z = \infty$) reflects all the power with no phase change ($\rho = +1$), and termination with $Z = Z_0$ absorbs the power ($\rho = 0$). The problem with a single coil probe may therefore be summarised in Fig. 19. The probe impedance has to be transformed to say 50 Ω to match the coaxial cable, and hence obtain power from the transmitter when the latter is on; and to 800 Ω say to noise match to the pre-amplifier when the transmitter is off. Thus the probe impedance must first be transformed, using one of the circuits already discussed, to 50 Ω resistive, and there must be provision in the pre-amplifier for transformation (hopefully without addition of extra noise) from 50 Ω to 800 Ω (for our particular example) in order to obtain the best noise figure. The protection may then be added in a variety of ways[14,15,16] of which two will be discussed. The first is shown in Fig. 20. Consider initially the case when the transmitter is off. The crossed diodes may be considered as open circuits. The probe impedance is transformed by C and C' to 50 Ω and the signal is carried along the cable to the pre-amplifier where M, X and Y transform it so that the effective source impedance is not 50 but 800 Ω. Inductance M must, of course, have as high a Q as possible and inevitably its resistance and that of the coaxial cable must degrade the signal-to-noise ratio slightly, though with a well constructed system this should be by no more than about 10%. When the transmitter is on, the diodes conduct, so protecting the FET, and one end of capacitor X is thereby effectively grounded by the diodes across M and the 1nF capacitor. Now the reactance of capacitor X is given by

$$\frac{j}{2\pi\nu_A X} \simeq j\sqrt{Z_0 R_N} \tag{19}$$

where R_N is the source resistance of 800 Ω required for the optimum noise figure and Z_0 is the cable impedance of 50 Ω. Thus the reactance of X is, in this example, $j200$ Ω. This, being effectively across the coaxial cable, introduces a slight mismatch between the transmitter and the probe, but for all practical purposes, it can be ignored, and so there is a direct path between the transmitter and the probe and the latter is power matched to the 50 Ω coaxial cable.

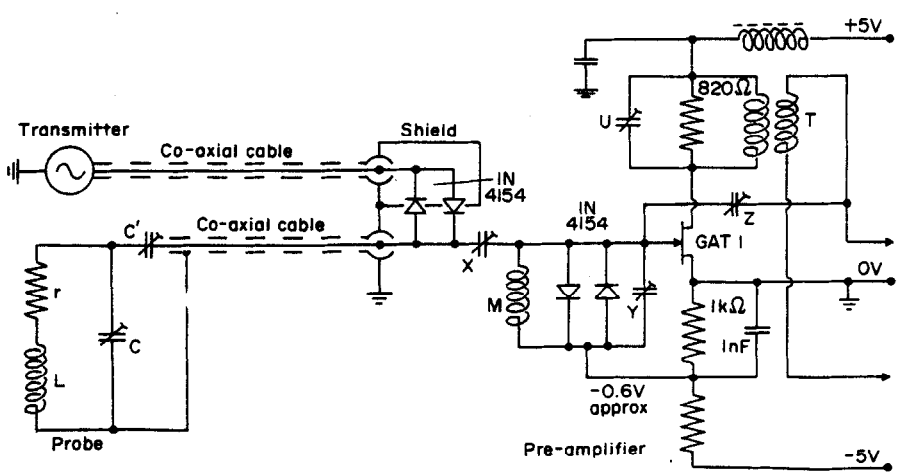

FIG. 20. A single-coil probe, and the first stage of pre-amplification, showing a method of protection.

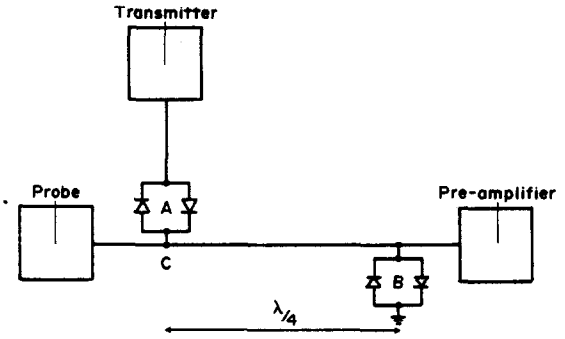

FIG. 21. Pre-amplifier protection using a $\lambda/4$ co-axial line.

The second method, which can be inconvenient at low frequencies, involves the use of a quarter wavelength line and again a pre-amplifier with transformation in its input so that its optimum source impedance is 50 Ω resistive. The circuit is shown in Fig. 21. As usual, when the transmitter is off, there is a direct path between the probe and pre-amplifier and diodes A, being an open circuit, isolate the transmitter. However when the transmitter is on, diodes B act as a short circuit across the line, and protect the pre-amplifier whilst reflecting the power with a phase change of 180°. The reflected wave thus returns to point C having suffered a 360° phase change and so, once equilibrium has been established, the quarter wavelength line can be ignored. The $\lambda/4$ line effectively transforms the short circuit at B to an open circuit at C. Of course at low frequencies, the $\lambda/4$ line is inordinately long (e.g. 12.5 m at 4 MHz) and can introduce unacceptable noise, but at higher frequencies the system works well. It fails when the inductance and capacitance of the diodes produce appreciable reactance, and in some circumstances, this may arise at frequencies as low as 100 MHz.

5. FREQUENCY CHANGING

Having lifted the signal from the probe out of the noise danger area with the pre-amplifier, we must now consider how to process the signal so as to give sensible results. The Larmor frequency is much too large to allow direct acquisition by, for example, a computer, and so an obvious step is to subtract, from the various frequencies issuing from the pre-amplifier, the frequency used to drive or irradiate the nuclear resonances, as this is readily available. Let us consider therefore two common methods of frequency changing.

5.1. *Mixers*[17]

The principle behind a mixer is quite simple. If two alternating voltages are applied to a device whose current versus voltage curve is non-linear, the non-linearity will mix the two signals and create, amongst other related frequencies, the sum and difference frequencies. Consider the practical case of a diode being used as the mixing device. Let the signal be $A\sin\omega_0 t$ and let the reference (the other voltage) be $B\sin\omega_r t$. Now the current passed by a diode is given by

$$I = I_0\left\{\exp\left(\frac{eV}{kT}\right) - 1\right\} \tag{20}$$

where I_0 is a constant ($\sim 10^{-6}$ A) and V is the applied voltage. Then

$$I = I_0\left\{\frac{eV}{kT} + \frac{1}{2!}\left(\frac{eV}{kT}\right)^2 + \ldots\right\}$$

and

$$V = A\sin\omega_0 t + B\sin\omega_r t$$

Let us consider the contribution to I from the second order term. After some algebra

$$V^2 = \frac{A^2 + B^2}{2} - \frac{A^2}{2}\cos 2\omega_0 t - \frac{B^2}{2}\cos 2\omega_r t + AB\cos(\omega_0 - \omega_r)t - AB\cos(\omega_0 + \omega_r)t \tag{21}$$

and thus the current through the diode contains the required frequency. Now it might be thought that the use of a mixer is a good method of detecting directly the signal in a continuous wave experiment for if we

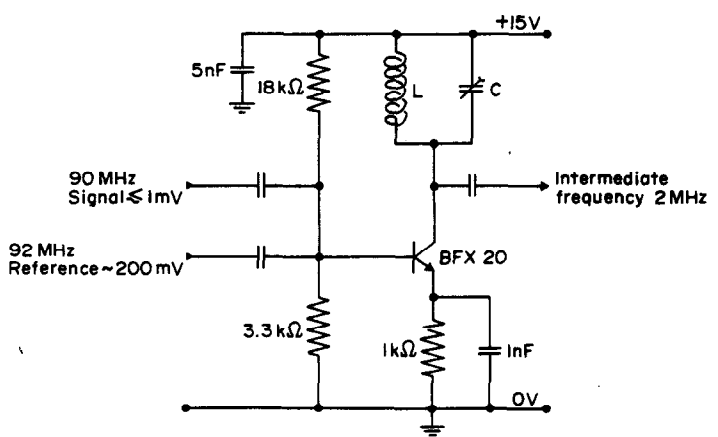

FIG. 22. A transistor mixer for a 90 MHz signal with 2MHz intermediate frequency. The reference could also have been 88 MHz.

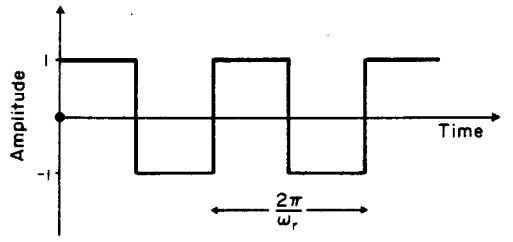

FIG. 23. The reference function for a phase-sensitive detector.

set $\omega_0 = \omega_r$, the direct part of the current becomes dependent on AB. However there is also a dependence on $A^2 + B^2$ which is non-linear in the signal A. Thus to linearise the output, B must be made very much larger than A. We are then attempting to detect AB in the presence of B^2 and the measurement of a small quantity in the presence of a large one is never a good idea for it makes great demands on the stability of the latter. In general the condition $B \gg A$ must always hold if other forms of distortion (see Section 11.2) are not to be present, and so a mixer may only be used to change to a frequency which is "not low". (A definition of "not low" is higher than the frequency bandwidth of any random fluctuations in B^2.) A typical mixer is shown in Fig. 22 where the diode characteristics of the emitter-base junction of a transistor provide the necessary square-law response, the current is collected from the collector of the transistor and the component at the intermediate frequency $(\omega_0 - \omega_r)$ (the IF) is selected by the tuned circuit LC.

5.2. *Phase Sensitive Detectors*

If it is necessary to change the frequency to a very low value, as will ultimately be the case, a phase sensitive detector must be used. This is a device which multiplies the signal alternately by ± 1, the frequency of alternation being the reference frequency ω_r. To appreciate how such a system works, consider first a Fourier analysis of the waveform of Fig. 23, which is the multiplicand at frequency ω_r. We have that

$$F(\omega) = \frac{4}{\pi} \sum_{r=1}^{\infty} \frac{\sin(2r-1)\omega_r t}{2r-1}. \tag{22}$$

Let us now include phase as well as frequency in the signal so that the latter is given by $\xi = A\sin(\omega_0 t + \sigma)$. Then after the multiplication we have that

$$\xi F(\omega) = \frac{2A}{\pi} \sum_{r=1}^{\infty} \frac{\cos\{(\omega_0 - [2r-1]\omega_r)t + \sigma\} - \cos\{(\omega_0 + [2r-1]\omega_r)t + \sigma\}}{2r-1} \tag{23}$$

and we can see that whenever the condition $\omega_0 \sim (2r-1)\omega_r$ is fulfilled there is a low frequency component which can be picked out. Normally of course, the first harmonic ($r = 1$) is used, in which case $\omega_0 \sim \omega_r$, but in the author's case, the third harmonic ($r = 2$) is used.[8] It might be wondered from whence the name of such a device arises, and this may easily be seen if we set $\omega_0 = \omega_r$, $r = 1$. The constant output is given by $(\xi F(\omega))_{DC} = (2A/\pi)\cos\sigma$ and we can see that the output is *sensitive* to the *phase* difference between the signal and the reference. Figure 24 shows a typical RF phase sensitive detector (PSD). Consider first the effect of the reference. During the first half of a cycle, current is driven through the transformer T_1 and via ACB. Diodes AC and CB are conducting whilst diodes AD and DB, being the other way round, are not. By symmetry, point C is at ground potential E, whilst point D is at whatever the potential set by the signal makes it—D is floating. Now on the second half of the reference cycle, the current, being in the opposite direction, flows through BDA making D ground and C floating. Points D and C are therefore alternately grounded. Looking at the transformer T_2 on the signal side, we must now consider what this alternate grounding does to the potential at F. The potential difference between C and F is the same as between F and D; namely ξ. Thus when C is grounded, the potential at F is $+\xi$. On the other hand, when D is grounded, the potential at F is $-\xi$ relative to ground. We have therefore accomplished our objective in multiplying the signal alternately by ± 1 at the reference frequency. For the above argument to hold, the signal must be very much smaller than the reference and negligible current must be drawn from terminal F, a point which

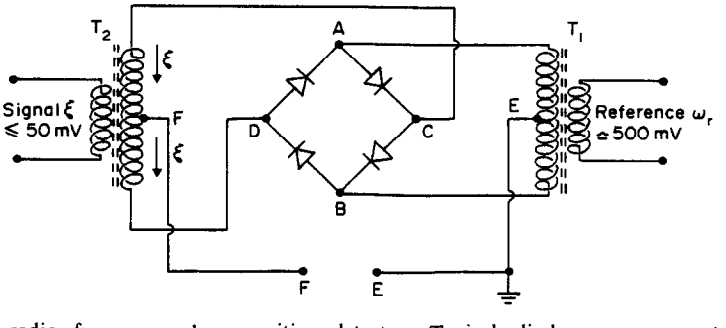

FIG. 24. A radio frequency phase-sensitive detector. Typical diodes are a matched quad of HP-5082-2970.

is frequently overlooked. Excess signal, as in the case of the mixer, produces distortion (see Section 11.2). At audio frequencies, transistorised circuits are normally used for phase sensitive detection rather than transformers and diodes, but the principle of operation ($\times \pm 1$) is exactly the same. Also, at frequencies less than about 30 MHz, PSDs capable of handling much larger signal voltages (~ 1 V) can be made and these can be used to advantage, as will be shown.

5.3. *Intermediate Frequency and Direct Amplification*

Most spectrometers are designed to operate with more than one nuclear species, and given a constant magnetic field, this means that operation at more than one frequency is necessary. Thus a separate probe and pre-amplifier is required for each species if optimum sensitivity is to be retained. If a little sensitivity may be sacrificed, then probes and pre-amplifiers covering several nuclear species can be used,[18] but whatever the situation, we must still be able to handle a range of frequencies which, in the extreme with the latest superconducting magnets, can cover nearly 500 MHz. Clearly a separate entire receiver for each frequency is uneconomical and the traditional approach to the problem is that after pre-amplification, the signal, whatever its frequency, is mixed with a suitable reference and "down converted" (as a first step in subtracting the transmitter frequency) to some standard intermediate frequency e.g. 2 MHz or 10 MHz etc. The resulting IF signal, which may originate from any nucleus, is then amplified to a manageable level (e.g. 1 V) before being processed further. Needless to say, the generation (unless a frequency synthesizer is employed) of all the necessary frequencies can be a tedious and complicated business and each manufacturer has his own way of performing the contortions required.

A more recent approach takes advantage of modern technology, for it is now possible to produce wideband amplifiers (~ 800 MHz) which can cope with the entire frequency range. Such an amplifier can follow the pre-amplifier(s), and direct phase sensitive detection with the circuit of Fig. 24 can then take place. There are advantages and disadvantages to both systems, particularly when pulsed methods are used. The tuned IF amplifiers tend to "ring" after the pulse for a long time (e.g. 80 μs) whereas the wideband amplifiers have negligible ringing and the signal is therefore available much sooner. On the other hand, it is much easier to change remotely the gain of a low frequency amplifier than it is that of a broadband system and this is a very important consideration when one considers the range of concentrations which is examined. (The question of dynamic range will be discussed a little later.) Probably the best compromise is a broadband intermediate frequency amplifier with a bandwidth greater than 1 MHz. However, let us now look a little more closely at the choice of intermediate frequency, when one is used.

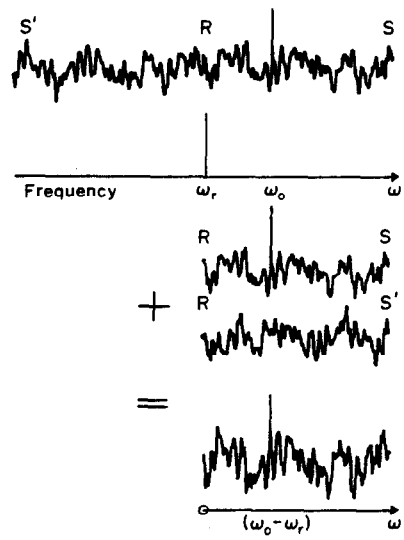

FIG. 25. Noise imaging.

5.4. *Noise Imaging*

Whenever a mixer or PSD is used to change frequency, the information, as to which of the two frequencies involved (signal and reference) is the higher, is lost. Thus for example in eqn (21), we have that the intermediate frequency is given by $AB\cos(\omega_0 - \omega_r)t$. This is the same as $AB\cos(\omega_r - \omega_0)t$, all we detect is the absolute frequency of the difference. Now in general, whenever we throw away information, we lose signal-to-noise ratio unless special steps are taken to avoid the loss. To show how this loss occurs, consider frequency changing the signal and noise whose spectrum is shown in Fig. 25. The signal is at frequency ω_0 and the reference at frequency ω_r. After the change of frequency, noise in the range R to S covers exactly the same range as noise in the range R to S'. Thus whilst we have only one *signal* at the intermediate frequency, we have *two* sets of noise—the noise in the range R to S' is effectively imaged in frequency ω_r, and, as noise *powers* add, the signal-to-noise ratio is decreased by a factor of $\sqrt{2}$. How then can we overcome this loss? There are two methods, one of which is commonly used and another which is rarer but rather instructive. The first method relies on the fact that the pre-amplifier is tuned and therefore passes signal and noise from the probe only over a limited bandwidth which is less than the value of the intermediate frequency. This is shown in Fig. 26. Although imaging still occurs, there is negligible noise to be imaged in the range R to S' and so the signal-to-noise ratio is preserved at the intermediate frequency.

The second method is more subtle and works by cancelling the imaged noise over a limited bandwidth.[19] It is termed single sideband detection (SSB) and relies upon detection in quadrature. Let us suppose that the signal is split and fed to two mixers or PSDs and that a 90° phase difference is introduced

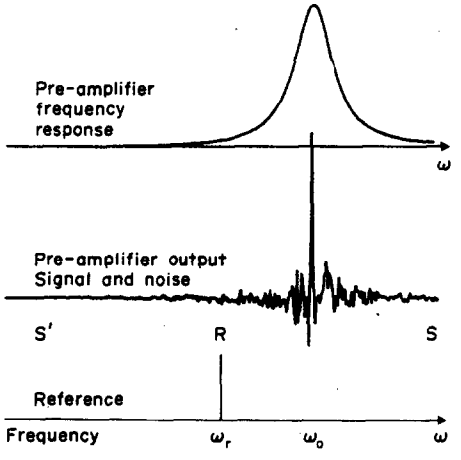

FIG. 26. Image rejection by pre-amplifier tuning.

either into one of the signals or one of the references. Then from eqn 23 we have that the output of the first frequency changer is given by

$$\psi_1 = \alpha \cos([\omega_0 - \omega_r]t + \sigma)$$

and of the second by say

$$\psi_2 = \alpha \cos([\omega_{0_0} - \omega_r]t + \sigma - 90°)$$

where α is a constant or

$$\psi_2 = \alpha \sin([\omega_0 - \omega_r]t + \sigma).$$

As has been remarked earlier for the case of two orthogonal receiving coils, detection in quadrature preserves the sign of the frequency information, and we can, as before, write the signal in complex notation to show this more clearly. Hence

$$\psi = \psi_1 + j\psi_2 = \alpha \exp j([\omega_0 - \omega_r]t + \sigma) \quad (24)$$

and the direction of rotation is dependent on whether ω_0 is greater or smaller than ω_r. The forms of ψ_1 and ψ_2 are shown explicitly for the two cases in Fig. 27 and obviously, with the particular phases chosen, ψ_2 changes sign when ω_r becomes greater than ω_0. Suppose now we delay ψ_2 by a quarter of a period, as shown. A comparison of ψ_1 and ψ_2-delayed shows that they are in phase for $\omega_r > \omega_0$ and out of phase for $\omega_r < \omega_0$. Thus if ψ_2-delayed is subtracted from ψ_1, any signal or noise from the region *RS'* of Fig. 25 is cancelled and we retain our signal-to-noise ratio. A block diagram of a single sideband detection scheme is shown in Fig. 28. It must be realised, however, that such a system can only work adequately over a bandwidth of about 20% of the intermediate frequency as it relies on a delay of a quarter of a period. The delay in time is fixed; frequency is variable and so a delay of $\pi/2|\omega_0 - \omega_r|$ is only obtainable for one frequency. In other words, *perfect* cancellation of the imaged noise occurs for only one frequency also. However, a 20% bandwidth is quite large and in many cases, this means that the IF can be as low as 1 MHz. The main advantage of SSB detection is, of course, that it can be used in conjunction with a broadband pre-amplifier whilst still retaining sensitivity.

5.5. *Pre-amplifier Gain*

In our consideration of frequency changing so far, we have observed that the signal entering the mixer or PSD must not be greater than some value if distortion of the intermediate frequency signal is not to occur. We have not considered, however, how *small* the signal may be before the sensitivity is degraded. Mixers and PSDs tend to be noisy devices with a noise figure of typically 10 dB. Thus

$$F = 10 = 10 \log_{10} \left\{ \frac{N_F^2 + N_S^2}{N_S^2} \right\} \quad (25)$$

where N_S is the noise associated with the source resistance of whatever is feeding the signal to the device, and N_F is the noise contributed by the device. In this application F is normally defined for a source resistance of 50Ω. Hence, from eqn (25), $N_F \simeq 3 N_S$ and it follows therefore that the gain of the pre-amplifier,

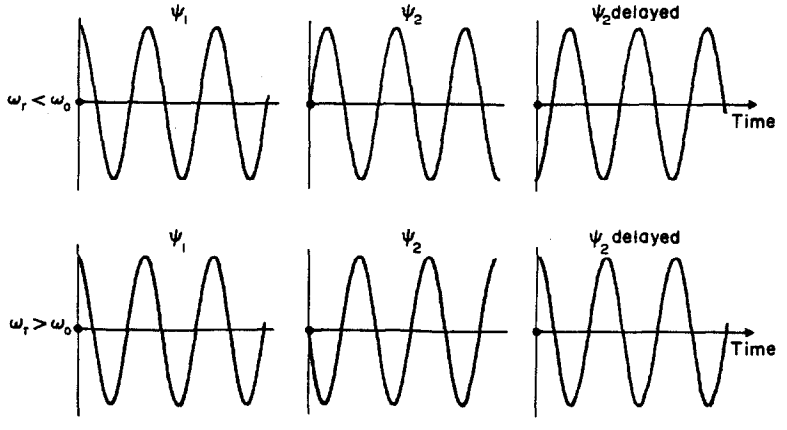

FIG. 27. The phase of the various signals in a single sideband detection scheme.

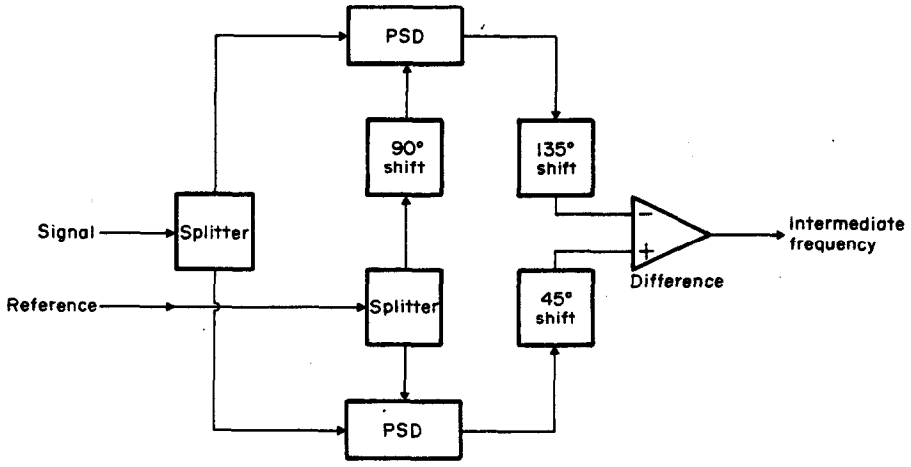

FIG. 28. A single sideband detector. The use of 45° and 135° phase shifters increases the bandwidth of the circuit as $d\phi/dv$ is the same for both shifts.

assuming it is working from a 50 Ω source at room temperature (i.e. the probe impedance has been transformed to 50 Ω resistance) must be $\gg 3$ if the noise from the mixer is to be negligible. One must beware, however, of making the gain too large or unacceptable loss of dynamic range will occur. As an example, consider the case of a spectrum containing broad peaks (e.g. 1 kHz wide) where the peak of interest is much smaller than the largest, and comparable with the noise. In a Fourier transform experiment, the height of the absorption peak is given by AT_2 where T_2 is the spin–spin relaxation time and A, the initial amplitude of the free induction decay, whilst the noise is given by (assuming convolution) $\sqrt{W_n 2T_2}$. The term W_n is the mean square RF noise voltage per unit bandwidth. Hence, *in a single* scan, the dynamic range is $D = A(T_2/2W_n)^{1/2}$ for this particular spectrum. Now after the pre-amplifier, $A \leqslant 30$ mV say in order not to overload the frequency changer, whilst $W_n = 4\alpha^2 kTR$, where α is the gain of the pre-amplifier and R is the source resistance which in our example is 50 Ω. The maximum dynamic range available is thus

$$D \leqslant \frac{3 \times 10^{-2}}{2\alpha} \sqrt{\frac{T_2}{2kTR}} \qquad (26)$$

and setting $T_2 = 3 \times 10^{-4}$ s and $R = 50\,\Omega$, we find that

$$D \leqslant \frac{2.91 \times 10^5}{\alpha}.$$

Thus for a dynamic range of 10^3, the pre-amplifier gain should not be more than 100 and this is a fairly typical value. In this context, it is of interest to note that the dynamic range of a proton spectrum of an aqueous solution can be larger than 10^5 and, quite obviously such a large range cannot be accommodated without gross distortion.

6. AUDIO FREQUENCY SIGNAL PROCESSING

6.1. *Detection*

Following the RF detection, we have an IF voltage which may be as large as 20 mV or as small as the noise, say 60 μV for a pre-amplifier gain of 100 and an IF bandwidth of 1 MHz. The signal, whatever it may be, must now be amplified to a level suitable for the final detection which completes the process of subtraction of the irradiating frequency from the Larmor frequency. If the IF is low enough, that level may be as large as 1 V, in which case an IF gain of between 50 and 20,000 is required, depending on the signal strength available. Unfortunately, certain spectrometers have a fixed IF gain which restricts considerably the versatility of the machine. Strong signals may overload the final detection stage, causing distortion, whilst weak signals may require excessive audio frequency gain. This in turn, if the output amplifiers are directly coupled may be the cause of baseline drift. However, assuming that all is well, the IF detection process follows much the same lines as the RF detection considered previously, and in particular, the considerations relating to signal-to-noise ratio and noise imaging apply in exactly the same manner. Unless precautions are taken, the sensitivity is degraded by a factor of $\sqrt{2}$ in a single detection and either the bandwidth of the intermediate frequency amplifier must be limited or two detections in quadrature phase must be made.

It is at this point that the broad design of the receiver becomes dependent upon the type of experiment being performed. Now, there is a vast variety of NMR experiments but it is convenient from the electronics viewpoint to divide them into two classes: firstly those experiments which in a time of the order of $5T_2$ (or $5T_2^*$, where T_2^* is the magnet inhomogeneity time constant) cause only one frequency of interest to be issued from the IF detection stage (for

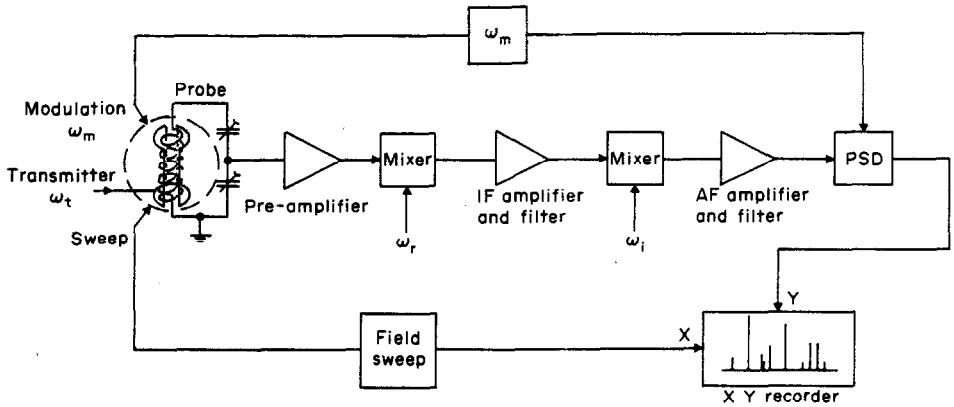

FIG. 29. A block diagram of a CW receiver employing field modulation. ω_t is the transmitter frequency. ω_r is the radio reference frequency, ω_i is the intermediate frequency and ω_m is the modulation frequency.

example a CW experiment), and secondly, those which, in the same time, cause many frequencies to be issued. This division is clearcut because in the second case, a computer is needed to sort out, with the aid of a Fourier transform, the various frequencies present, whereas in the first case, no computer is needed. Let us consider then these two cases.

6.2. *The Continuous Wave Experiment*

If we irradiate the nuclear system with a single continuous frequency, we can expect the receiver to pick up the response of the system at that frequency, plus leakage of the irradiation from the transmitter to the receiving coils. Subtraction of the irradiating frequency therefore leaves us with a direct voltage issuing from the IF detection stage which comprises mostly leakage with a small contribution from the nuclei. Now the leakage can change with such vagaries as temperature, humidity etc. and detection of the small nuclear signal in the presence of large leakage is therefore not a good idea. We must devise a means of discriminating between the nuclear signal and the leakage. This is commonly done in two ways: field modulation,[20] or pulse modulation[21,22] which also is termed, rather unfortunately, time-sharing. The aim of both methods is to make the Larmor frequency differ from the irradiation frequency by an amount equal to the modulation frequency ω_m, and as an added advantage, the method of pulse modulation also reduces the leakage by a large factor. The full details of both methods lie outside the scope of this article; from our point of view, the important fact is that the signal of interest issuing from the IF detection stage is no longer a direct voltage, but rather an alternating voltage which may have a frequency (normally equal to the modulation frequency) between 50 Hz and 100 kHz, depending upon the particular application. Thus to avoid noise imaging, as before, either the IF bandwidth must be less than the modulation frequency and centred on, e.g. $\omega_0 + \omega_m - \omega_r$, or a single sideband detection must be employed. A subtle third possibility which has much to commend it, is to make the intermediate frequency equal to the modulation frequency. In this case however, SSB detection at the radio frequency must be employed as it is not feasible to make a pre-amplifier with a bandwidth sufficiently narrow to avoid noise imaging. Figure 29 shows a block diagram of a typical CW spectrometer where the noise imaging is avoided by the use of bandwidth limiting. In Fig. 30 we can see how the signal and leakage are processed in order to reject the leakage. The spectrum is observed by sweeping the main magnetic field B_0, which of course varies the Larmor frequency ω_0. Energy is absorbed by the nuclei when ω_0 is equal to the transmitter frequency plus the field modulation frequency, and the probe and pre-amplifier therefore receive a signal at frequency ω_0 plus leakage at fre-

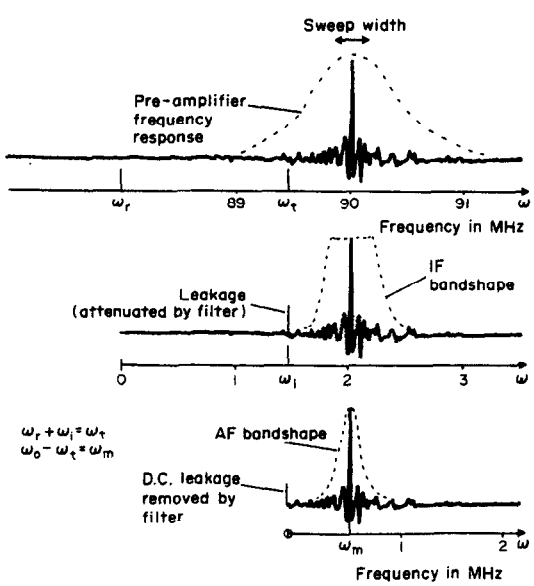

FIG. 30. The various frequency changes in the spectrometer receiver showing how bandwidth limiting stops noise imaging and reduces the leakage.

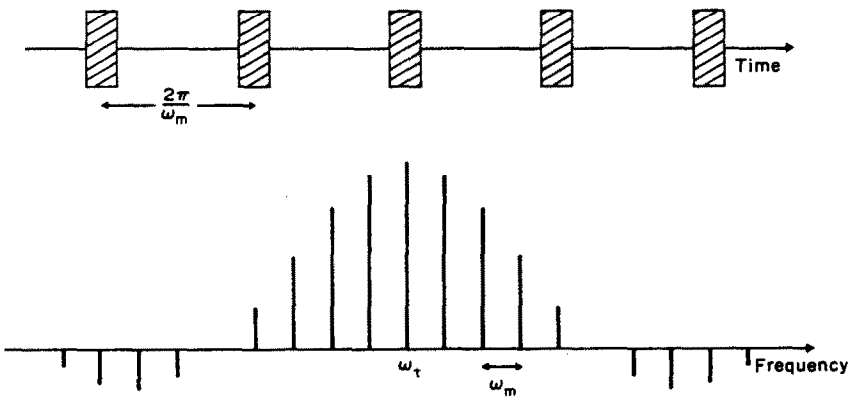

FIG. 31. Pulse modulation and its frequency spectrum. ω_m must be greater than the spectral width.

quency ω_r. After the radio frequency detection, the leakage is outside the pass band of the IF amplifier and therefore is attenuated severely whilst the signal, being somewhat higher in frequency, is not. After the intermediate frequency detection, the leakage is reduced to zero frequency, whilst the signal, which retains its full sensitivity, is at frequency ω_m, the modulation frequency. It is therefore a simple matter to reject the leakage and finally detect the frequency ω_m to get an output proportional to the signal. It might be added that the method of detection outlined above is but one of several, for in general whenever a frequency change is made, the reference can be above or below the signal frequency; it is the difference which is defined. Thus ω_t could be given by $\omega_0 + \omega_m$. Another possibility is to increase the field modulation, irradiate at the Larmor frequency ($\omega_t = \omega_0$) and detect at frequency $\omega_0 \pm \omega_m$. Full details are given in reference (20).

When pulse modulation is used, the transmitter is turned off for most of the time, whilst signal is received, but periodically it is turned on for a few microseconds giving rise to pulse modulation as shown in Fig. 31. The frequency spectrum is also shown and it is clear that the nuclei are irradiated whenever the condition $\omega_0 = \omega_t + r\omega_m$ is fulfilled, where r is an integer. Thus the conditions of Fig. 30 may also be fulfilled, for whatever leakage there is will be at the transmitter frequency, whilst the signal may be at some other frequency.

With regard to the final phase sensitive detection at frequency ω_m, the noise output of the detector is determined of course by the following filter, (see Fig. 29) being proportional, from eqn (10), to the square root of the bandwidth. The signal however, assuming the nuclear system is in equilibrium with the driving irradiation, is constant and so the signal-to-noise ratio can be increased as desired until the limit of stability of the transmitter power, the receiver gain etc. is reached. Now of course the spectrum must be swept, and if the final filter has a bandwidth of $\Delta\nu$ it takes a time $\sim 5/\Delta\nu$ to reach a new equilibrium state. Hence the greater the signal-to-noise ratio required, the longer it takes to sweep the spectrum. Ernst[23] has analysed in detail the optimum value of the filter for a given sweep rate so the subject will not be pursued further here, but there *is* one point of interest with regard to the effect of the final phase sensitive detection upon the noise. If the filter bandwidth is $\Delta\nu$ we have from eqn (10) that the noise is given by $N_{RMS} = \sqrt{W_n \Delta\nu}$ where W_n is the mean square noise per unit bandwidth. This is incorrect in this particular case, for there is no way in the final detection that we can avoid noise imaging. For example noise at frequency $\Delta\nu/10$ comes from frequencies $\omega_m \pm 2\pi\Delta\nu/10$ prior to the detection and the final noise is thus given by $N_{RMS} = \sqrt{2W_n\Delta\nu}$. One might ask therefore: "Where is the information loss associated with the imaging?" The answer is, as usual, that detection in quadrature restores the lost information. However, the output of the second phase sensitive detector is the dispersion mode spectrum which is less amenable to interpretation and we therefore *choose* to lose the information contained in it.

6.3. *The Fourier Transform Experiment*

If the nuclear system is perturbed by short pulses of radio frequency energy at frequency ω_t and repetition period greater than $5T_2$, the entire system is stimulated simultaneously, and we obtain a free induction decay as a signal whose Fourier transform is the spectrum of interest.[24] As usual, we wish to subtract the irradiation frequency ω_t from the Larmor frequencies ω_{0i}, but, unlike the CW spectrometer of Fig. 29, the IF detector must be a PSD as we wish to change frequency to an audio frequency range which can include direct voltages. The audio signals must then be accumulated in the memory of a computer, prior to Fourier transformation. Now clearly, if we are to avoid confusion in the spectrum, the transmitter frequency ω_t must be completely to one side of the spectrum. If this is not the case, when we subtract ω_t from the Larmor frequencies, a line at frequency $\omega_{01} = \omega_t + \omega_a$ could be confused with one at frequency $\omega_{02} = \omega_t - \omega_a$. Of course, if the crystal filter of Fig. 30 were included in the IF ampli-

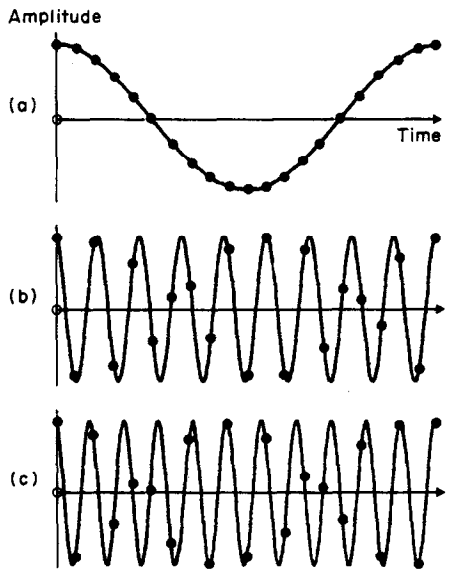

FIG. 32. The effects of sampling every 500 μs on signals at (a) 100 Hz; (b) 900 Hz; and (c) 1100 Hz.

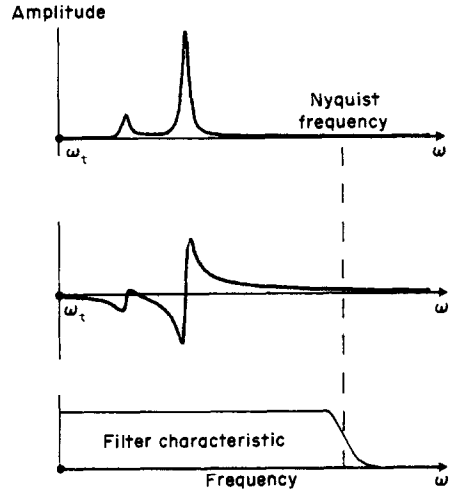

FIG. 33. The correct choice of Nyquist frequency and filter cut-offs prevents aliasing.

fier there would be no confusion; one would lose lines whose frequencies were less than ω_t, but there would also be a $\sqrt{2}$ improvement in signal-to-noise ratio, for the noise at frequencies less than ω_t would also be lost and there would be no noise imaging. Let us assume then for the time being that we are dealing with a spectrometer similar to that already described, that the transmitter frequency is to one side of the spectrum and that a crystal filter is employed to prevent noise imaging in the final detection. (Let us however also bear in mind that quadrature detection preserves frequency information and obviates the need for a crystal filter—a point to be discussed later.) How do we transfer the signals to the computer, and what does a Fourier transform do?

A computer is a digital device; it cannot record a variable continuously; rather it periodically takes a sample, and the effects of this sampling are similar in some ways to phase sensitive detection. Figure 32 shows three different frequencies sampled at the same rate. Whilst it is obvious that the low frequency is sampled correctly, we can also see that the samples taken from the signal at 0.9 kHz are identical with those taken from the signal at 1.1 kHz. This effect is referred to as "aliasing" and is very similar to the noise imaging already discussed, for, with a sampling rate of 500 μs per point, noise at a frequency of 1.1 kHz will appear in the computer as noise at 0.9 kHz and so degrade the sensitivity. This effect, first pointed out by Nyquist,[25] is known as the Nyquist sampling theorem and the latter states that the maximum frequency which may be stored without aliasing (the Nyquist frequency) is given by $\nu_{max} = 1/2\delta$ where δ is the interpoint time. It follows that δ must be small enough to accommodate the entire spectral width and secondly, there must be a filter, prior to the computer, which cuts off all noise at a frequency greater than ν_{max}. It is not generally realised how good this filter must be. For example, an ordinary RC filter whose cut-off frequency (−3 dB point) is set to the Nyquist frequency allows enough noise to be aliased to reduce the sensitivity by nearly 30%. A sharp cut-off filter, such as a Butterworth filter[26] is required if maximum sensitivity is to be retained. Another point, frequently overlooked, is that the Nyquist frequency must be sufficiently large to include not just the spectral width as defined by the *absorption* spectrum, but rather the width as defined by the dispersion spectrum whose wings, it may be remembered, fall off more slowly with frequency than do those of the absorption mode. If this precaution is not observed, the baseline of the absorption spectrum may contain aliased wings from the dispersion mode.[27] The situ-

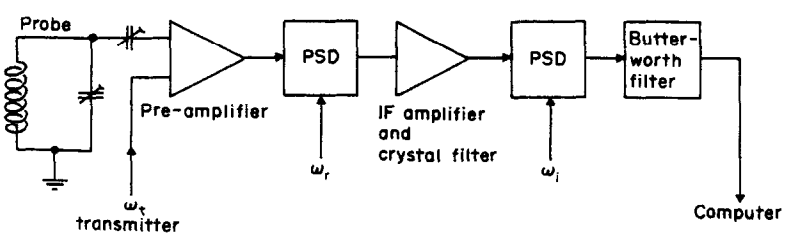

FIG. 34. A typical Fourier transform spectrometer receiver.

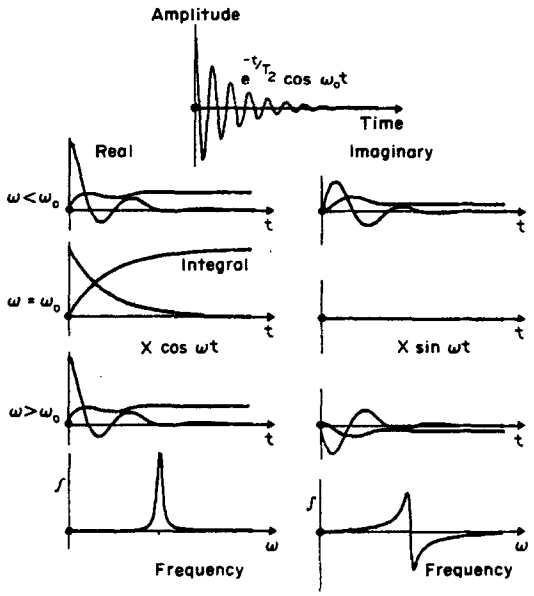

FIG. 35. Fourier transformation. Products and integrals for various values of ω are shown.

ation is summarised in Fig. 33, and reference (28) contains further information on the use of computers in NMR, including digitisation errors and dynamic range problems. Figure 34 shows a block diagram of a typical FT spectrometer receiver and problems discussed in more detail in Section 11 include recovery of the receiver from the overload generated by the large pulse power, and dynamic range, which is a much more serious problem in Fourier transform experiments than in CW experiments as distortion can generate spurious spectral lines.

A useful physical insight into what a Fourier transformation does can be had by considering the mathematics bit by bit. A definition of a Fourier transformation useful in NMR is

$$F(\omega) = \int_0^\infty F(t)\,e^{-j\omega t}\,dt \qquad (27)$$

Here, $F(\omega)$ is the spectrum, $F(t)$ is the free induction decay, and the real part of $F(\omega)$ is the cosine transform whilst the imaginary part is the sine transform. Consider first the product $F(t)\,e^{-j\omega t}$, and for clarity, let $F(t) = \cos\omega_0 t\,e^{-t/T_2}$. Then the product $F(t)e^{-j\omega t}$ may be envisaged as a phase sensitive detection in quadrature with reference frequency ω. We may ignore the high-frequency components of the product; it is the difference frequency which contributes to the integral, and Fig. 35 shows the low frequency product for several values of ω, together with the integrals. The computer in effect performs the final phase sensitive detection and filtering of the CW spectrometer of Fig. 29 together with a frequency sweep. The signal-to-noise advantage of the Fourier experiment, however, comes from the fact that data from the whole spectral width are accumulated simultaneously, and only at the end of the experiment is the Fourier "sweep" performed, whereas with a CW experiment only one frequency at a time is observed.

6.4. *Quadrature Detection*[29]

By now, the principle of information preservation by quadrature phase sensitive detection should be highly familiar, and Fig. 36 shows the final stages of a receiver equipped with such detection. The figure also shows the two audio signals passing to the X and Y deflections of an oscilloscope. Figure 37 shows three Lissajous figures so obtained with free induction decays. The X and Y deflections correspond exactly to the graphs in Fig. 35 and the change in the direction of rotation as the transmitter frequency passes through the Larmor frequency is strikingly obvious. As has been pointed out in eqn (24), the free induction decay can now be written in complex notation as

$$F(t) = \alpha e^{-t/T_2} \exp j([\omega_0 - \omega_r]t + \sigma) \qquad (28)$$

where the real part corresponds to the X deflection and the imaginary part to the Y deflection. The phase σ is the angle made with the real (X) axis. From eqn (27) the Fourier transform of the complex free induction decay is given by

$$F(\omega) = \int_0^\infty \alpha\, e^{-t/T_2} \exp j([\omega_0 - \omega_r]t + \sigma)\, e^{-j\omega t}\,dt \qquad (29)$$

and if this expression is expanded, it may be seen that there is a direct analogy with the single sideband

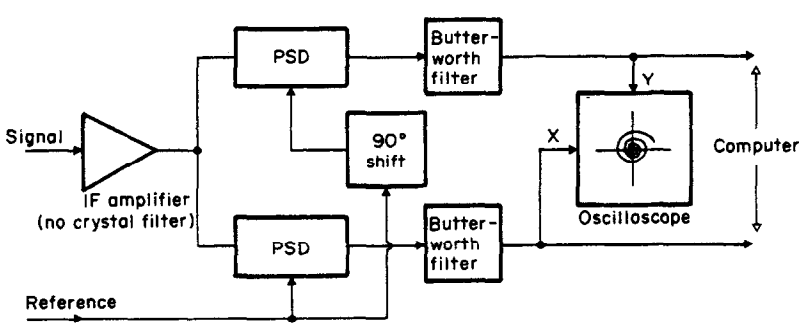

FIG. 36. A quadrature detection system for a Fourier transform spectrometer. As frequency information is preserved, no crystal filter is needed.

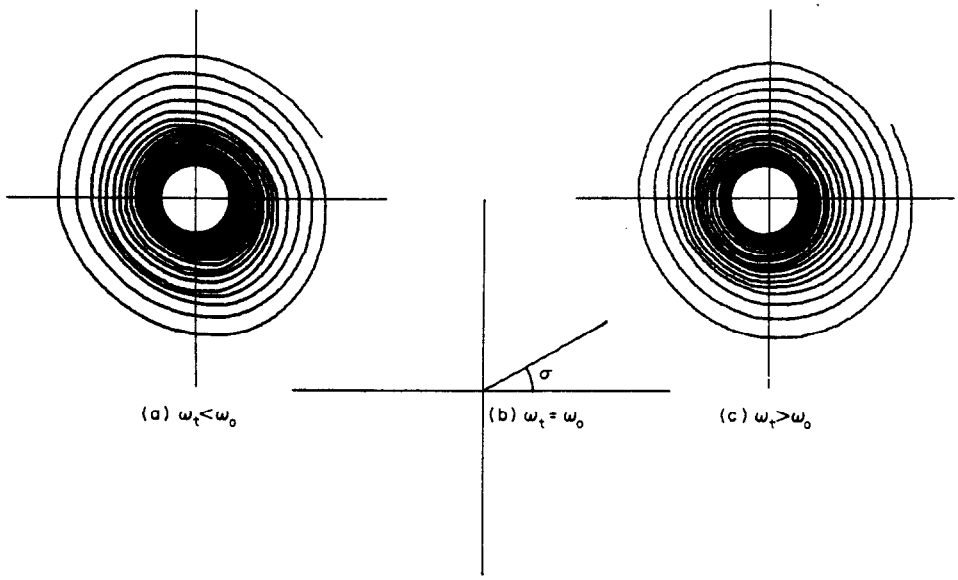

FIG. 37. Lissajous figures obtained with quadrature detection: (a) ω_t, the transmitter frequency is less than the Larmor frequency ω_0; (b) $\omega_t = \omega_0$; and (c) $\omega_t > \omega_0$.

detection scheme mentioned earlier. Equation (28) represents the two quadrature signals of Fig. 28; multiplication by $\cos\omega t$ gives rise to no phase shift, but multiplication by $\sin\omega t$ corresponds to a 90° delay, and of course this holds for any value of ω, *including negative values*. If we let

$$\Delta\omega = \omega_0 - \omega_t - \omega$$

eqn (29) becbmes

$$F(\omega) = \int_0^\infty \alpha \exp\left\{\left(-\frac{1}{T_2} + j\Delta\omega\right)t + j\sigma\right\} dt$$

$$\therefore \quad F(\omega) = \alpha e^{j\sigma}\left\{\frac{1}{1/T_2 - j\Delta\omega}\right\} \qquad (30)$$

which is the complex formula for a Lorentzian line. After the appropriate rotation (phase correction) of $-\sigma$, the real part is the absorption curve whilst the imaginary part is the dispersion curve. Of course, all the above analysis relies on the two phase sensitive detections being exactly in quadrature phase, the two filters being exactly matched and the gains of the two audio channels being identical right through to the computer memory. This is never the case, and this problem, which gives rise to imaging about zero frequency, is discussed in Section 11.3. To summarise then, quadrature detection enables the sensitivity of the receiver to be fully utilised and as frequency information is preserved, the transmitter frequency may be set in the middle of the spectrum. Even though two free induction decays are accumulated, no extra memory is needed as the Nyquist frequency may now be one half of what it was previously.

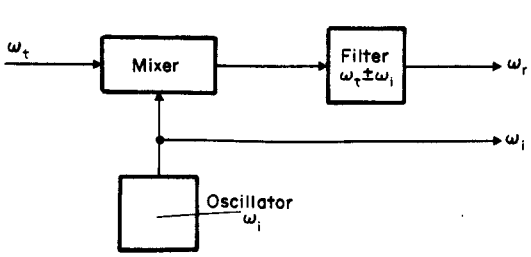

FIG. 38. Reference frequency generation by mixing.

7. REFERENCE FREQUENCY GENERATION

The principle of subtracting the transmitter frequency from the Larmor frequency has been a major theme throughout much of the preceding sections and the condition $\omega_r + \omega_i = \omega_t$ has been established in Fig. 30, i.e. when an intermediate frequency is employed, the two reference frequencies must, obviously, add up to the transmitter frequency. The subject of phase however has been to a large extent judiciously ignored as it adds little to the understanding of the receiver. In practice, phase stability is of great importance; it would for example be exceedingly annoying if, during a CW sweep, the phase of the signal altered from the absorption to the dispersion mode, and in practice, also, phase and frequency stability are intimately linked as the former is the integral of the latter. It follows that it is insufficient to derive for example, ω_r, from a stable oscillator. Rather it must be derived from ω_t by subtraction of ω_i. Thus ω_i may wander slightly in phase or frequency but ω_r compensates so that $\omega_r + \omega_i$ is always a constant equal to ω_t. Figure 38 shows one method of generating ω_r and ω_i. A mixer or modulator is used, and as usual, amongst other frequencies, the sum and difference frequencies are generated. The required oscillation can be picked out by a filter whose band-

width is $\ll \omega_i$ and the circuit of Fig. 22 can be readily adapted for the purpose, the collector circuit being tuned to either $\omega_i \pm \omega_i$ as desired. The SSB circuit of Fig. 28 can also be adapted in the same manner for generation of a sum or difference frequency and this circuit is useful when the value of ω_i is too low to permit filtering of the desired signal. Both types of circuits preserve phase coherence and so are essential whenever frequency changing is employed. Finally, it might be added that when continuous wave spectroscopy is employed, there *must* also be a phase coherence between the modulation and the reference ω_m for the final PSD of Fig. 29.

Such then is the working of most spectrometer receivers, and we now proceed to consider certain aspects in more detail.

8. THE PROBE SENSITIVITY

Most aspects of probe design are covered in a consideration of three topics: sensitivity, homogeneity and recovery. Whenever more than one of these attributes is desirable, compromises are essential and the purpose of this section is to indicate the various considerations involved and the conflicts in design which may arise. In addition, one or two minor topics such as double-tuning and crossed-coil design are briefly considered.

8.1. *The Coil*

As has been shown already, the signal induced in the receiving coil is proportional to the B_{1xy} field at the sample generated by unit current flowing in the coil, whilst the noise power is proportional to the resistance r of the coil. Thus to optimise the signal-to-noise ratio, B_{1xy} must be maximised whilst the resistance is minimised. In general, these two processes are in conflict, and so the ratio $B_{1xy}/\sqrt{r}$ is a slowly varying function. For example, if we double the number of turns of a coil, B_{1xy} is doubled, but as the radius of the wire used has to be halved to fit in the same space, r increases by a factor of four: $B_{1xy}/\sqrt{r}$ therefore remains constant. The factors under consideration are more subtle and concern proximity effect[30] and self-capacitance.

The flow of electric current is invariably associated with the generation of a magnetic field, and at high frequencies the alternating magnetic field produced induces in turn EMFs in the conductor which ensure that the current flows only on the surface of the conductor (see for example reference (31)). Hence at frequencies greater than a few megahertz, current flows down a wire in a thin skin on the surface, the current density decreasing exponentially as one penetrates the surface. The average depth is given by

$$\delta = \sqrt{\frac{2\rho}{\omega\mu\mu_0}} \tag{31}$$

and for copper at 100 MHz, $\delta = 6.6\ \mu$m. The term ρ is the resistivity of the conductor and μ the permeability. This "skin effect" increases substantially the resistance of a conductor in comparison with its zero frequency value, but when several conductors are in close proximity, it is also responsible for other changes. The skin effect may be summarised crudely by the realisation that where there is no alternating magnetic field, there is no alternating current. Thus if several conductors each have the same alternating current flowing down them, as shown in Fig. 39, there will be regions of zero field and hence zero current. This "proximity effect" increases further the resistance of conductors in close proximity by a factor which is very difficult to calculate; it may be between one and ten but is typically three.

If we consider therefore the simplest of receiving coils, a solenoid, there will be some optimum separation of the turns which gives the best ratio $B_{1xy}/\sqrt{r}$. As indicated in Fig. 39, this separation is about three times the wire radius[32] and, fortunately, it is easy with a solenoid to obtain experimentally a measure of the ratio. Because a solenoid is a relatively closed structure most of the energy stored in the B_1 field is away from the wire, and hence the stored energy is a good measure of the square of the B_{1xy} field at the sample. However, as the energy stored is also a measure of the inductance, it follows that at any one frequency, the Q of the coil is a measure of the signal-to-noise ratio obtainable. An independent indication of this fact is obtained when one remembers that the inductance of a solenoid is virtually independent of the radius of the wire used. For a Helmholtz or saddle-shaped coil however, which has a far more open structure, this is not the case and Q is a very poor indication of sensitivity. For another example of Q being an unreliable guide to sensitivity, see Section 8.3 on double tuning. Decreasing the radius of the wire used in such a coil may hardly affect the Q as the energy stored in the field close to the wire increases (in contrast to the energy stored in the field over the sample which stays the same) along with the resistance which also increases. The sensitivity therefore *decreases* and the best way of assessing a design for saddle-shaped coils is an NMR experiment!

However for solenoids, the Q *is* a good measure, and it transpires that the highest Q values are obtained when the separation of the wires is about

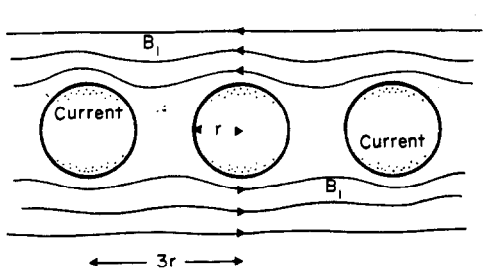

FIG. 39. The current distribution associated with proximity effect.

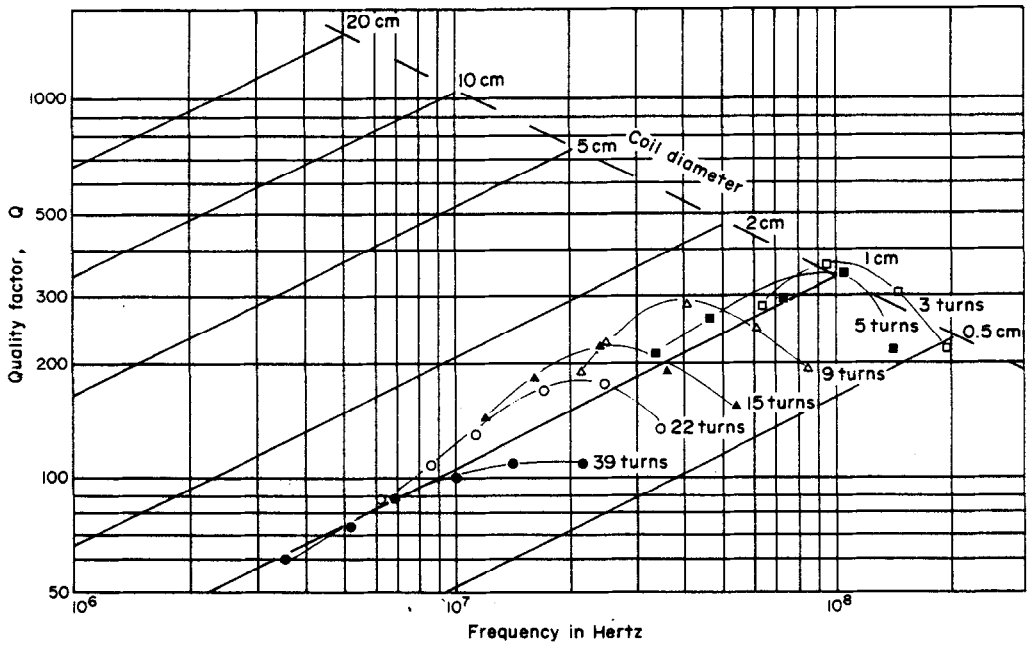

FIG. 40. A plot of Q versus frequency for a set of solenoids. The detailed plot is for a set of coils 1 cm in diameter and length. The spacing of the turns is three times the wire radius. Q is approximately given by the formula $Q = 3.5d\sqrt{\nu}$ where d is the coil diameter in metres and ν is the frequency in hertz. The broken line marks the upper frequency limit, above which the number of turns tends to unity and the quality of the coil deteriorates.

three to four times their radius and the length of the coil is a little less than its diameter.[30] Now of course one must take into account that such a shape may not utilise fully the available volume of homogeneous B_0 field and it may well be desirable to extend the length of the solenoid. The increase in sample volume will easily offset the loss of Q in such cases.

We must next consider how many turns to put on our solenoid. At first sight, this does not seem to matter very much. However, there are limits; at the lower end, the resistance of the coil must be very much greater than those of the leads to the tuning capacitor and of the latter itself, whilst at the upper end, self-capacitance between the turns of the coil must not be so large as to induce phase changes which cause the EMFs induced in one part of the coil partially to cancel those induced in another part. Unfortunately, because noise *powers* add, the noise does not cancel in the same way. Figure 40 shows an experimental plot of Q versus frequency for a set of coils, all of the same overall dimensions, with varying numbers of turns. From eqn (31) one would expect $Q = \omega L/r$ to vary as $\omega^{1/2}$ and this may be seen to be broadly true. However, as one progresses to higher frequencies, each curve drops away from the $\omega^{1/2}$ line and this behaviour marks the onset of self resonance (caused by the self capacitance[33]) and the upper limit of usefulness of the coil. At these upper frequencies, the tuning of the coil is especially sensitive to changes in the self-capacitance, and these may be caused by changes in the temperature of the coil and, more importantly, changes in the sample. The probe becomes "sample sensitive" to a degree which is unacceptable. A plot of Q versus frequency is therefore essential if one is to be sure that a coil is suitable for a particular frequency range and this particular test can also be applied to Helmholtz coils which, due to the greater length of conductor per unit configuration, require fewer turns. A word of warning is required here concerning the measurement of Q at different frequencies. The easiest method of measuring the Q is to resonate the coil at the frequency of interest and measure the Q of the tuned circuit. The capacitor has of course been selected to

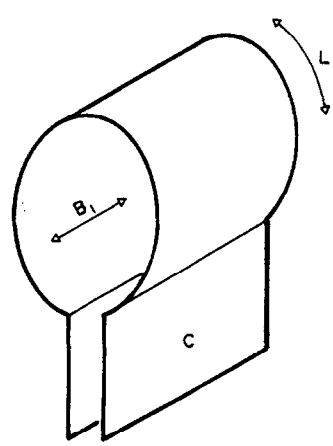

FIG. 41. A single-turn solenoid.

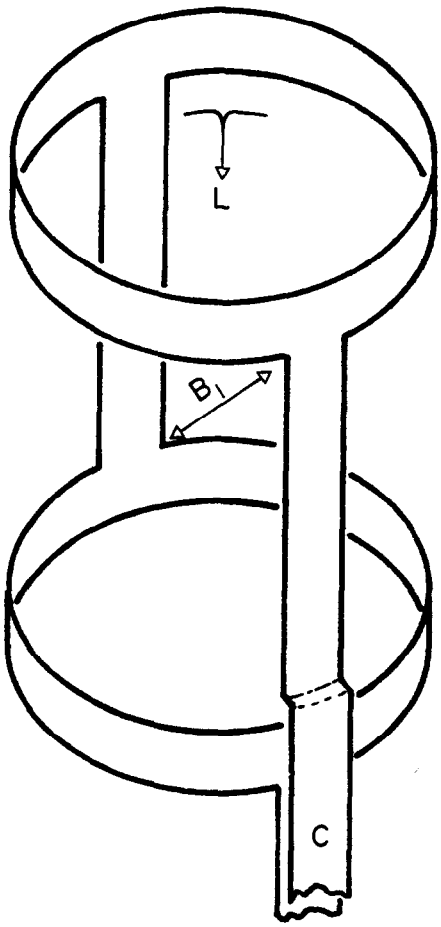

FIG. 42. A single-turn saddle-shaped coil.

have a Q very much greater than that of the coil. However when a variable capacitor is opened, the current flows through a smaller surface area, and the Q falls rapidly. This effect can cause an artificial falling away of the Q versus frequency curve and it is advisable therefore to check capacitors prior to use. A simple way of doing this if the coil is wound of copper is to immerse the latter in liquid nitrogen whilst keeping the capacitor at room temperature. The resistivity of copper at 77 K is approximately one tenth that at room temperature and so, from eqn (31), the Q should increase by a factor of over three if the Q of the capacitor is high. If one wishes, the capacitor Q may be approximately measured by this technique.

As one progresses to higher frequencies, the number of turns on a coil tends to zero and greater care has to be taken to keep the leads to the capacitor short. Also, geometrical considerations dictate the use of foil rather than wire. Thus for a 1 cm coil, Q values at frequencies above 100 MHz tend to be a little lower than one would expect from an extrapolation of Fig. 40. The ultimate in this process is the design of Fig. 41 which resonates up to 600 MHz with Q values in the region of 300. The equivalent design for use with a superconducting magnet is shown in Fig. 42 and this configuration, due to Dadok,[34] is useful to about 450 MHz with Q values again in the region of 300. The sensitivity of this type of coil is about one half that of a solenoid at the same frequency and is somewhat better than the more conventional saddle-shaped coil (used with superconducting systems at lower frequencies) shown in Fig. 43.

Obviously, the conductor chosen should have the highest possible conductivity and silver is therefore an obvious candidate. However, paramagnetic impurities tend to destroy the main field homogeneity and for this reason, annealed, high purity copper is generally preferred. Its resistivity at room temperature is only a few per cent greater than that of silver, and so the loss in sensitivity is negligible. However, at lower temperatures, copper is appreciably better and at 77 K is twice as conducting as silver at zero frequency.

At microwave frequencies, cavities are employed as resonators and it is possible to use such techniques at lower frequencies with the aid of dielectric loading. Lafond[35] pioneered the design of these devices, but the Q value of the system published by Kan *et al.*[15] is only seventy, giving a signal-to-noise ratio at 250 MHz for 1% ethylbenzene of 160. This is rather low. It is also possible at high frequencies to tune a coil of the type shown in Fig. 42 not with the capacitance C, but rather with a length of co-axial line. If the line is of solid construction with very low losses, the extra resistance added is small, and the system does have the advantage that it can be tuned well away from the coil at the end of the line. The distinction between this type of construction and a cavity becomes increasingly blurred as one progresses to higher frequencies. Yet another variant on the cavity theme is the use of a slotted waveguide.[36]

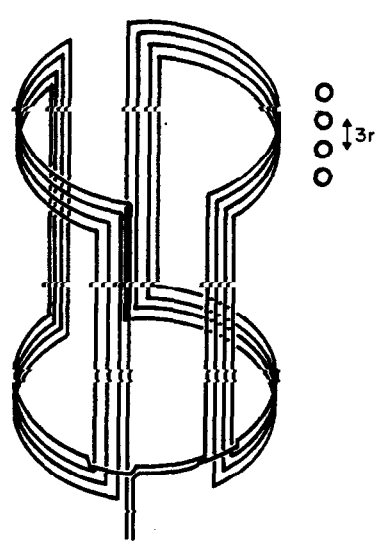

FIG. 43. A saddle-shaped coil for use at frequencies less than 80 MHz.

8.2. *The Surroundings*

So far, the receiving coil has been considered in isolation. In practice it has to be mounted, and shielded so that it does not receive radiation from the outside world. Considerable losses can be caused if the mounting and shielding are not correctly performed and these losses are of three types; magnetic, electric and electromagnetic (radiative). The simplest to understand is magnetic loss. If a conductor is in close proximity to the receiving coil, the magnetic field generated by the coil can induce eddy currents in the conductor which heat the latter. This energy dissipation mechanism therefore lowers the effective Q of the coil and correspondingly, when signal is received, noise is also received from the coupling to the conductor. This effect can be particularly important if the conductor is at a much higher temperature than the receiving coil as the noise contribution is then also much higher. It follows that any conductor must be well removed from the coil and a rule of thumb is "at least twice the largest dimension of the coil away". Of course, if the *sample* is conducting, there are problems. Naturally, any shield should be made of a good conductor such as copper so as to reduce the losses as far as possible.

Turning now to electric losses, these occur primarily in dielectrics subject to electric fields generated by the coil and its associated capacitors. Probably the most lossy dielectric is the sample itself and whilst it is difficult at high frequencies to shield electrostatically the *coil* from the sample (due to the distributed capacitance that any shielding introduces) attention can certainly be paid to the *leads* from the coil. This is particularly important with high frequency coils, for the leads are often of large surface area to minimise inductance and resistance. In such cases, it is advisable to screen the "hot" lead from the sample with the "cold" lead, and a useful insulator in this context is "Teflon" tape as its dielectric properties, though not quite so good as air, are excellent. Figure

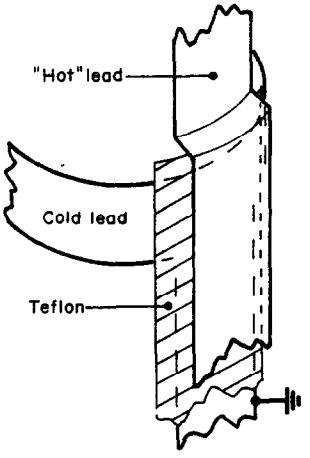

FIG. 44. A detail from the design of a foil, saddle-shaped coil, showing how dielectric loss is minimised.

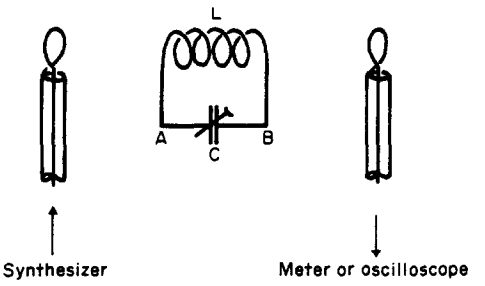

FIG. 45. Measurement of Q at very high frequencies.

44 shows a detail of the construction of a high frequency saddle-shaped coil. In addition to providing shielding, this type of construction also generates a high Q fixed capacitor in parallel with the variable version, and this can often be useful when the desired total capacitance is between convenient commercially available values.

The terms "hot" and "cold" have just been referred to, and these vague, though commonly used terms (along with "ground" for "cold") need to be explained in more detail, for it is not at all obvious what "ground" means at frequencies where a short length of wire has sufficient inductance to present a considerable impedance to the passage of current. Now it might be thought that "ground" is simply a large volume of conductor with a capacitance much greater than those associated with any circuitry. Presumably in such a situation, the potential of that conductor is constant. To show that this is not so, consider the apparatus of Fig. 45 which can be used very successfully to measure Q values at high frequencies. The tuned circuit (LC) is *loosely* and symmetrically coupled to a frequency synthesizer on one side and a meter or oscilloscope on the other. The Q is measured from the bandwidth of the transfer function at the -3 dB (70%) points, and is the ratio of the centre frequency to the bandwidth. Now suppose we "ground" point A or B by attaching the outer braiding of a co-axial cable, in preparation for connecting to the tuned circuit via a matching capacitance C'. Despite the fact that a large volume of conductor has been attached, the measured Q can drop dramatically with just the braiding connected. This is due, quite simply, to radiation from the cable and this effect is particularly severe as the cable length approaches $\lambda/4$—a quarter wavelength. Obviously, in this context, the term "ground" can be thoroughly misleading, and we need a more accurate definition when considering how to shield a probe coil and connect to it.

In the author's opinion, the most useful approach is first of all to consider how a shield works. As the sample has to be placed in the receiving coil, a shield is invariably open ended, and so let us assume that the probe is mounted inside a conducting tube, preferably copper. At the frequencies of interest in NMR, the wavelength of irradiation is very much greater

than the cut-off wavelength of the tube, considering the latter as a waveguide.[37] Thus any propagated irradiation is attenuated according to

$$V = V_0 \exp\left(-\frac{2\pi x}{\lambda_c}\right) \tag{32}$$

where λ_c is the cut-off wavelength. For a circular tube of diameter d, the largest cut-off is that of the TE_{11} mode and is given by $\lambda_c = 1.707\,d$. Thus

$$V = V_0 \exp\left(-\frac{3.68x}{d}\right) \tag{33}$$

or, the propagated wave is attenuated at the rate of 32 dB per unit length. An immediate result is that a shield four times its diameter in length will reduce pick-up by a factor of over one million *provided* that there is no conductor running down the inside of the shield. If there is, e.g. a piece of co-axial cable, the outer braiding of the latter and the shield form in themselves a co-axial line which can transmit RF voltages very satisfactorily, rendering the shield useless. Now obviously, there has to be a connection to the probe, so how can the co-axial line be taken up the shield without providing a path which introduces leakage and which also correspondingly dampens the probe Q by allowing radiation to escape from the shield? If the outer braiding on the cable is connected to the shield, as shown in Fig. 46, any incident radiation is reflected, and the coupling to the waveguide decreases as the impedance of the connection tends to zero. The ultimate in this process is a disc of metal across the shield, through which the inner conductor protrudes. The left-hand side of the disc and the shield may then be considered radiation free, and truly at "ground", and the connection from the probe coil is then made to the disc or shield with a conductor having negligible inductance. This system works well; it provides excellent shielding and, correspondingly, maintains the probe coil Q. However, it does have the disadvantage that access to the probe from the right hand side of Fig. 46 is impossible. An obvious solution is to make the co-axial braiding a part of the shield as shown in Fig. 47. This allows access to the probe and once again, prevents leakage.

8.3. *Double Tuning*

Double tuning a coil allows two nuclear species of widely differing Larmor frequencies to be irradiated or observed simultaneously whilst retaining

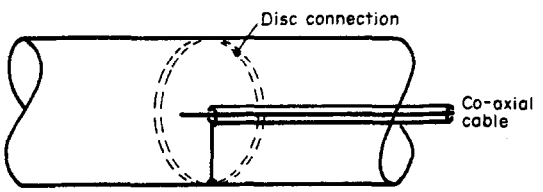

FIG. 46. Reflection of radiation in a probe shield.

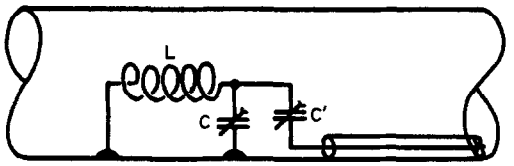

FIG. 47. Elimination of a co-axial construction prevents leakage.

identical B_1 field distributions. However, unless care is taken, the sensitivity of the higher frequency signal can easily be impaired; that of the lower frequency signal invariably is. A typical double-tuned circuit is shown in Fig. 48, the two frequencies corresponding to protons and deuterium. One must now ask how the addition of inductance M effects the signal-to-noise ratio of the proton signal. Presumably the probe L has been wound so as to retain a high Q and so inductance M will have a Q no higher. It follows that the addition of M does not affect significantly the measured Q of the proton probe. Thus,

$$\frac{1}{Q_{\text{total}}} = \left(\frac{L}{L+M}\right)\frac{1}{Q_M} + \left(\frac{M}{L+M}\right)\frac{1}{Q_L}$$

However, a little algebra soon shows that the proton sensitivity is reduced by a factor

$$\rho_H \simeq \left\{1 + \frac{Q_L}{Q_M}\left(\frac{L}{M}\right)\right\}^{-1/2} \tag{34}$$

where Q_L and Q_M are the Q values of the respective coils at 270 MHz. Once again it is clear that the measured Q is no indication of signal-to-noise ratio. Assuming that $Q_L = Q_M$, we can see from eqn (34) that $M \gg L$ if the sensitivity is to be retained, and a problem in the construction of M then arises for, in attempting to make M large, the latter may self-resonate. M is therefore best constructed by adding several inductors ($\sim L$) in series whilst ensuring that there is no coupling between them. Another commonly-used circuit adds a tuning capacitor across M in order to prevent 270 MHz entering the 41 MHz line. This circuit offers little advantage in sensitivity;

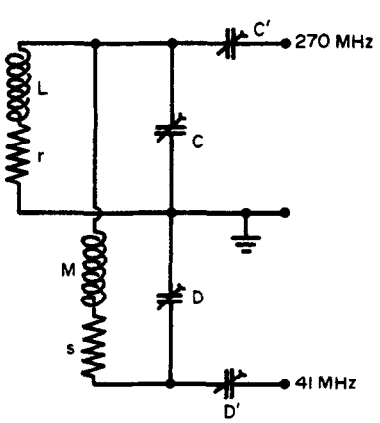

FIG. 48. A double-tuned probe circuit.

the addition of the extra capacitor merely changes the value of C. As far as the deuterium signal is concerned, the double tuning reduces its sensitivity by a factor

$$\rho_D \simeq \left\{1 + \frac{Q_L}{Q_M}\left(\frac{M}{L}\right)\right\}^{-1/2} \tag{35}$$

where the Q values are those measured at 41 MHz. For $M = 3L$, and assuming $Q_L = Q_M$, $\rho_H \simeq 0.87$ and $\rho_D \simeq 0.5$.

Preserving the sensitivity of the low frequency signal which may be desirable, for example in cases of proton decoupling, is considerably more difficult and is best accomplished with the aid of a crossed-coil probe. However, if a single-coil configuration is desirable, co-axial lines may be used to prevent the passage of certain frequencies or to produce a resonant circuit at two frequencies, and as such lines may be constructed with very high Q values if solid rods and tubes are employed, sensitivity may be but little impaired. Further details are given in reference (38).

8.4. *Crossed-Coil Configurations*[39,40]

The purpose of a crossed-coil system is usually to isolate the receiver from the transmitter. The receiver coil is therefore the inner of the two coils on the grounds that transmitter power is expendable but sensitivity is not. It is often thought that the greater size of the transmitter coil invariably leads to irradiating B_1 fields of better homogeneity. However, it must be remembered that the irradiating B_1 flux has to negotiate the receiving coil and the latter may disturb the homogeneity appreciably. Isolation of the two coils is approximately achieved by an orthogonal type of construction, which greatly reduces magnetic coupling. To reduce electrostatic coupling, a Faraday shield is often employed, but as was noted earlier this should not be too close to the receiving coil as it may lower the self-resonant frequency. When considering isolation, it must be borne in mind that both amplitude and phase are involved and therefore, as both magnetic and electrostatic coupling are present, one variable will in general be insufficient to cancel leakage from one coil to the other. Two independent variables are needed. An obvious possibility is rotation of the transmitter coil so that $B_{1_T} \cdot B_{1_R} \simeq 0$ can be varied (the subscripts refer to the two coils). Another variable may be obtained with the aid of "paddles".[39,40] In the case of Helmholtz coils, these are two small pieces of metal foil placed (diametrically opposite) between the two sets of coils. The eddy currents generated in the foil by B_{1_T} produce a field B_{1_P} whose phase is 45° different to that of B_{1_T}, and which couples to B_{1_R}. Thus by successive manipulations of the transmitter coil and the "paddle" positions a null may be obtained, resulting in an isolation of better than 60 dB.

An electronic, rather than mechanical, approach to the problem of leakage cancellation is to introduce into the receiver a small voltage of equal amplitude and opposite phase to that of the leakage. This may be executed in a variety of ways, a clever example of which is given in reference (41).

9. THE PROBE—HOMOGENEITY AND RECOVERY

9.1. B_0 *Homogeneity*

It is very easy to spoil the main field homogeneity by ignoring the magnetic susceptibility of materials used in the construction of the probe. If the sample is to be spun, a construction which aims to retain symmetry about the spinning axis is advantageous, as any inhomogeneity introduced is manifest in the spinning sidebands rather than the main line. Because NMR may employ highly homogeneous fields (~ 1 in 10^9) even the slightest change in susceptibility can have its effects; and impurities in the glass former used for mounting the coils, and in the coils themselves may have enormous effects on the lineshape. The susceptibility of quartz glass is -6×10^{-6} SI units which is not negligible and so to obtain good homogeneity, the coil former should be much longer than the coils and as thin as possible, particularly when an iron magnet is used. The same applies to the sample tube unless spherical samples are employed. As for the coils, the susceptibility of pure copper is -1.1×10^{-6} and it is sometimes advisable to reduce this value to zero. This may be done with the aid of rhodium plating ($\chi = +13.8 \times 10^{-6}$), a layer of approximate thickness $r/25$ being required on wire of radius r. However the technique is only viable when this thickness is very much less than the skin depth of the copper, for the conductivity of rhodium is three times worse that of copper, and thus at higher frequencies, the sensitivity of the spectrometer is adversely affected. In this case, copper may be plated on rhodium or some other paramagnetic metal. Typical commercial high purity copper contains 2 ppm iron and if this type of copper is employed at low fields considerable problems may be encountered. However, iron saturates at about 2 T and hence at higher fields it is often possible to select copper whose nett susceptibility is zero.

A major problem can be caused by paramagnetic tuning capacitors. At high frequencies, the capacitors must be close to the coil if lead resistance is to be minimised and this destroys the main field homogeneity. Non-magnetic high Q capacitors must therefore be used in such cases. Other possible sources of field perturbation include thermocouples, brass screws, leads on semiconductors and occasionally the sample itself.

9.2. B_1 *Homogeneity*

There is little to be said concerning the homogeneity of the field produced by a solenoid coil as the latter possesses axial symmetry. It is possible to improve the axial homogeneity by concentrating turns

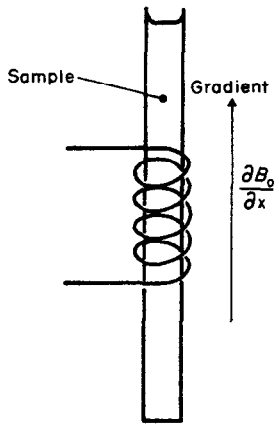

FIG. 49. A linear field-gradient enables one to observe the B_1 field inhomogeneity.

at the ends of the coil, but the effort involved and the loss of sensitivity rarely render this exercise worthwhile. In general, to obtain excellent B_1 homogeneity over the sample, the dimensions of the latter must invariably be less than those of the coil, and thus sensitivity is forfeited. An excellent measure of the B_1 homogeneity over an accurately known sample may be obtained with the aid of zeugmatography.[42] For example, suppose we wish to plot the axial B_1 field in a single-coil probe. A long sample, as shown in Fig. 49, is employed and a strong, linear field gradient is applied along the axis to distinguish different regions of the sample. The Fourier transform of the FID obtained from a *small* flip angle pulse, or a CW spectrum obtained with a power much less than saturation level, is effectively a plot of B_1^2 versus distance and a typical example is shown in Fig. 50. By using differently-shaped samples, plots may be obtained as desired. Other measurements are possible, and in particular Torrey's method of transient nutation[43,44] gives a plot of sample volume versus B_1 field.

The design of saddle-shaped or Helmholtz coils presents a rather difficult problem when homogeneity is considered, and unlike solenoidal receiving coils, the homogeneity is reflected in the spectra obtained, for the absence of complete cylindrical symmetry results, when the sample is spun, in sidebands which cannot be removed by "shimming" or greater spinning speeds. An insight into why this is so may be obtained with reference to Fig. 51 which is a crude plot of the B_1 field produced by saddle-shaped coils. Let us assume that the sample has been perturbed by a pulse of *small* flip angle at time $t = 0$. Then the elementary magnetic moment δM produced in volume δVs at point P is proportional to the field B_1 at that point and of course this proportionality also includes the phase of the precessing magnetic moment. Now when the signal is received, the induced EMF in the coils is given, from eqn (2), by;

$$\delta\xi = -\frac{\partial}{\partial t}\{B_1 \cdot \delta M\}$$

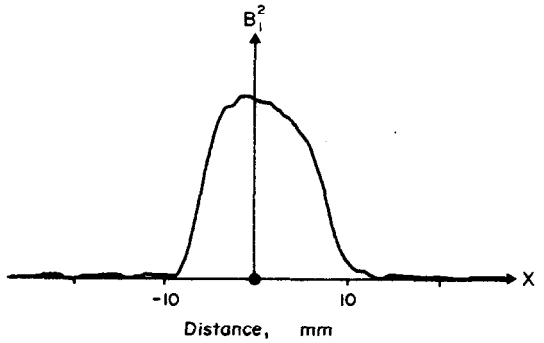

FIG. 50. The axial B_1 homogeneity of a saddle-shaped coil of length and diameter 10 mm.

or, if we employ complex notation,

$$\delta\xi = Rl - \frac{\partial}{\partial t}\{B_1\,\delta M^*\}. \tag{36}$$

Thus, for a *static* sample, we can see from eqn (36) that B_1 phase is unimportant—phase changes induced in transmission are mirrored upon reception, and the signal is simply proportional to $|B_1|^2$. However, for a *spinning* sample, this is not the case. To continue, we need a description of the B_1 field, and as magnetostatic potential obeys Laplace's equation, this is best obtained in terms of spherical harmonics. The magnetic field due to the various harmonics may be expressed fairly simply in cylindrical polar coordinates, and taking the z axis as the axis of symmetry, we shall be mainly interested in three harmonics: Y_1^1, Y_3^1 and Y_3^3. In the xy plane these three harmonics may be considered as the following fields:

$$\begin{aligned} B_1^1 &\propto e^{-j\phi} \\ B_3^1 &\propto r'^2(e^{j\phi} + 2e^{-j\phi}) \\ B_3^3 &\propto r'^2 e^{-j3\phi}. \end{aligned} \tag{37}$$

The real part of the field is directed as increasing radius r' a in Fig. 52) whilst the imaginary part is directed as increasing ϕ. To convert to Cartesian coordinates, one multiples by $e^{j\phi}$, but cylindrical polar coordinates are preferable as the exponent indi-

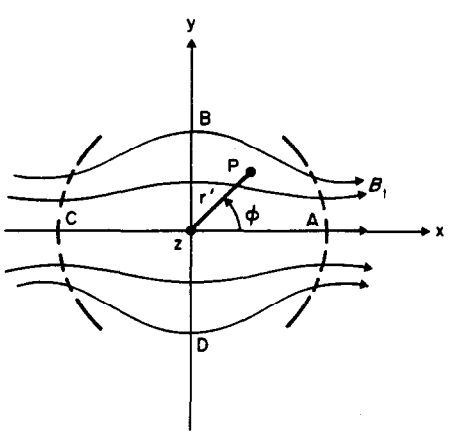

FIG. 51. The B_1 field produced by saddle-shaped coils.

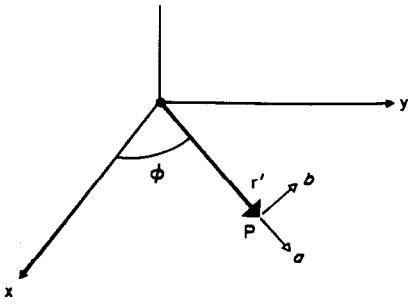

FIG. 52. Cylindrical polar coordinates, **a** and **b** are unit vectors.

cates the degree of the harmonic. Thus we can see that B_1^1 represents the main B_1 field directed along the x axis whilst the other harmonics represent inhomogeneities. Why these particular harmonics have been selected will become apparent later. Thus let

$$B_1 = \alpha e^{-j\phi} + \beta r'^2(2e^{-j\phi} + e^{+j\phi}) + \gamma r'^2 e^{-j3\phi} \quad (38)$$

where α, β and γ are constants of proportionality. At time $t = 0$, the magnetic moment at point P is given by

$$\delta M = MB_1 e^{-j\omega 0 t}\delta V_s \text{ where } \phi = \phi_0.$$

If sample spinning is now commenced, $\phi = \phi_0 + \omega_s t$ and as the Larmor frequency is independent of the spinning speed for dipolar and quadrupolar nuclei,

$$\delta M = M\{\alpha e^{-j\phi_0} + 2\beta r'^2 e^{-j\phi_0} + \gamma r'^2 e^{-j3\phi_0} + \beta r'^2 e^{+j\phi_0}\} \times e^{-j(\omega_0+\omega_s)t}\delta V_s$$

To obtain the complete signal, we must integrate over the entire sample, and as $dV_S = r'dr'd\phi_0 dz$, only those terms in the expression for $d\xi$ which are independent of ϕ_0 contribute. Thus

$$\xi = Rl - \frac{\partial}{\partial t}\int_{r'}\int_{z} 2\pi M r'\{[\alpha^2 + 2\alpha\beta r'^2 + 3\beta^2 r'^4]e^{j\omega_0 t} + \gamma^2 r'^4 e^{j(\omega_0 - 2\omega_s)t}\} dr' dz. \quad (39)$$

From eqn (39) we can see that the Y_3^3 harmonic produces a second order spinning sideband which is proportional to the square of the inhomogeneity and independent of the spinning speed. The asymmetry in the sidebands is due to the fact that the inhomogeneity introduces both amplitude and phase modulation. In practice of course, other inhomogeneities are present and the small angle pulse approximation is not valid, so sidebands are seen on both sides of the main line. (The lack of dependence on spinning speed is due to the fact that *phase* and not frequency modulation is present. With main field (B_0) inhomogeneity, frequency modulation is created, and as phase is the integral of frequency, an inverse dependence on spinning speed is manifest.)

We must now consider which design gives the best homogeneity. As the spherical harmonics form an orthonormal basis set, it should be possible to expand, in cylindrical coordinates, the field due to a saddle-shaped coil in powers of $e^{j\phi}$, and hopefully eliminate the Y_3^3 harmonic responsible for the spinning sideband. Consider the coil shown in Fig. 53 where the arcs subtend an angle α and the four verticals joining them run from $z = -f$ to $z = +f$. The fields in the xy plane due to unit current in the two arcs CF is derived from the vector magnetic potential and given at point P by

$$B_{1\,\text{arc}} = \frac{\mu\mu_0}{2\pi}\int_{-\alpha/2}^{+\alpha/2} \frac{af e^{-j(\alpha-\phi)} d\alpha}{[a^2 + f^2 + r'^2 - 2ar'\cos(\alpha - \phi)]^{3/2}}.$$

The denominator may be expanded by the binomial theorem for small values of r' and we obtain

$$B_{1\,\text{arc}} = \frac{\mu\mu_0 af}{2\pi(a^2+f^2)^{3/2}}\int_{-\alpha/2}^{+\alpha/2}\sum_{n=0}^{\infty}\sum_{p=0}^{n}\sum_{q=0}^{p} -\tfrac{1}{2}C_{nn}C_{pp}C_q\rho^{n-p}\sigma^p e^{j(p-2q+1)(\alpha-\phi)} d\alpha \quad (40)$$

where

$$\rho = \frac{r'^2}{a^2+f^2}, \quad \sigma = \frac{-ar'}{a^2+f^2}, \quad {}_fC_g = \frac{f!}{(f-g)!g!}.$$

Now if we consider the effect of the arcs DE, we note that their current direction is reversed from that of arcs CF and that they are displayed by 180°. The field they produce is therefore that of eqn (40) multiplied by $(-1)^{p-2q}$, and the total field due to the arcs

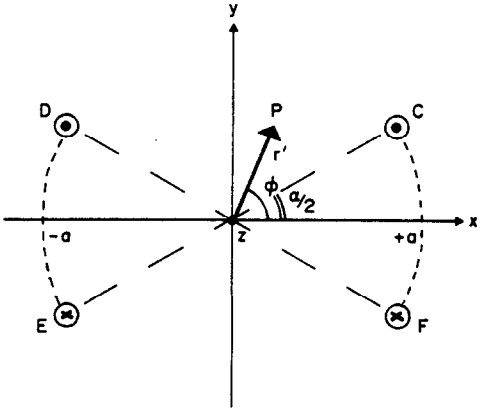

FIG. 53. The coordinates employed for a saddle-shaped coil. The four arcs of angular width $\alpha°$ are at heights $z = \pm f$.

has, as a result, only odd degree harmonics. The total arc field is therefore;

$$B_{1\,\text{arcs}} = \frac{\mu\mu_0 af}{\pi(a^2+f^2)^{3/2}} \sum_{n=0}^{\infty}\sum_{p=0}^{n}\sum_{q=0}^{p} -\tfrac{1}{2}C_{nn}C_{pp}C_q\rho^{n-p}\sigma^p e^{-j(p-2q+1)\phi} \times \sin\frac{(p-2q+1)\alpha}{2} \quad (41)$$

where p is an even quantity. From this expression we can see immediately that third degree harmonics can be cancelled by setting $\sin 3\alpha/2 = 0$ hence $\alpha = 120°$. Let us therefore examine the field from the four verticals in the hope that the same equality holds.

The vector magnetic potential at point P in the xy plane due to a vertical at angular position α is given by;

$$A = \frac{\mu\mu_0}{4\pi}\int_{-f}^{+f} \frac{dz}{[a^2+z^2+r'^2-2ar'\cos(\alpha-\phi)]^{1/2}}.$$

As before, the denominator may be expanded by the binomial theorem and we obtain

$$A = \frac{\mu\mu_0}{4\pi}\int_{-f}^{+f} \frac{1}{(a^2+z^2)^{1/2}} \sum_{r=0}^{\infty}\sum_{s=0}^{r}\sum_{v=0}^{s} -\tfrac{1}{2}C_{rr}C_{ss}C_v\tau^{r-s}\psi^s e^{-j(s-2v)\phi} e^{j(s-2v)\alpha} dz$$

where

$$\tau = \frac{r'^2}{a^2+z^2}$$

and

$$\psi = \frac{-ar'}{a^2+z^2}.$$

If we now observe the effect of all the verticals, it is clear that cancellation occurs when $(s-2v)$ is even, and so the total potential contains only odd degree harmonics. Thus

$$A_{\text{verticals}} = \frac{\mu\mu_0 k}{\pi}\int_{-f}^{+f} \frac{1}{(a^2+z^2)^{1/2}} \sum_{r=0}^{\infty}\sum_{s=0}^{r}\sum_{v=0}^{s} -\tfrac{1}{2}C_{rr}C_{ss}C_v\tau^{r-s}\psi^s e^{-j(s-2v)\phi} \times \sin\frac{(s-2v)\alpha}{2} dz \quad (42)$$

where s is odd and k is the unit vector in the z direction. Once again, third degree harmonics may be annulled by setting $\alpha = 120°$, and so it is firmly established that the angular width of saddle-shaped coils should be 120° for optimum homogeneity, so annulling third degree spherical harmonics, and in particular the harmonic Y_3^3.

We have not yet considered how the B_1 field varies with z away from the xy plane. The symmetry of the coil system ensures that only even order variations with z are permissible. The harmonic Y_1^1 has no variation in the z direction, and the lowest power harmonic present which *has* is Y_3^1. The full expression for the field (parallel to the xy plane) produced by this harmonic is

$$B_3^1 \propto z^2 e^{-j\phi} + r'^2(e^{j\phi} + 2e^{-j\phi}) \quad (43)$$

and if this harmonic could be cancelled by appropriate adjustment of the height $2f$ of the coils, the homogeneity in the z direction would be considerably improved. We need therefore to select from eqns (41) and (42) those terms of first degree which vary as $r'^2 e^{\pm j\phi}$, as they are a unique representation of the Y_3^1 harmonic present. The relevant terms from eqn (41) are the following;

$$B_{3\,\text{arcs}}^1 = \frac{2\mu\mu_0 af}{\pi(a^2+f^2)^{3/2}}\sin\left(\frac{\alpha}{2}\right) \times \left\{\left[\frac{15}{8}\left(\frac{ar'}{a^2+f^2}\right)^2\right]e^{j\phi} + \left[\frac{15}{4}\left(\frac{ar'}{a^2+f^2}\right)^2 - \frac{3}{2}\frac{r'^2}{a^2+f^2}\right]e^{-j\phi}\right\} \quad (44)$$

and these terms may be expressed, if desired, as sums of the two orthogonal harmonics Y_3^1 and $Y_3^{1'}$, where $Y_3^{1'}$ is given by eqn (43) rotated by 90°. The relevant term from eqn (42) is

$$A_{3\,\text{verticals}}^1 = \frac{\mu\mu_0}{\pi}\sin\phi\sin\left(\frac{\alpha}{2}\right)\left\{\frac{3afr'^3}{4(a^2+f^2)^{5/2}}\right\}k$$

$$B_{3\,\text{verticals}}^1 = \frac{1}{r'}\frac{\partial A}{\partial\phi} - j\frac{\partial A}{\partial r'}$$

in this instance, and hence

$$B_{3\,\text{verticals}}^1 = \frac{2\mu\mu_0 af}{\pi(a^2+f^2)^{3/2}} \times \sin\left(\frac{\alpha}{2}\right)\left\{\frac{3r'^2}{8(a^2+f^2)}[2e^{-j\phi} - e^{-j\phi}]\right\}. \quad (45)$$

Adding eqns (44) and (45) we see that the B_3^1 field may be eliminated by setting $f = 2a$. Thus to summarise, the best homogeneity is obtained from a saddle-shaped coil when its length is twice its diameter and its angular width is 120°. Unfortunately, such a sample shape rarely utilises to the full the volume of good B_0 homogeneity and it is usual to employ saddle-shaped coils whose length is about the same as the diameter, thereby sacrificing B_1 homogeneity.

Finally, we must consider what loss of signal occurs through restricting the angular width to 120°. From the equations above, it is simple to show that the Y_1^1 field is given by

$$B_1^1 = \frac{2\mu\mu_0}{\pi}\sin\left(\frac{\alpha}{2}\right) \times \left\{\frac{f}{a(a^2+f^2)^{1/2}} + \frac{af}{(a^2+f^2)^{3/2}}\right\}e^{-j\phi}. \quad (46)$$

The loss in sensitivity compared to $\alpha = 180°$ is therefore only about 13%, which in most applications is unimportant.

9.3. *Recovery*

In some experiments, the desired signal is a transient which lasts only a few microseconds after the end of a transmitter pulse, and in such circumstances, if the signal is to be observed, any ringing from the receiving coil and its tuning capacitor must decay very rapidly. Typically, the input of a receiver is overloaded for a time $5Q/\nu_0$ where Q is the quality factor of the coil and ν_0 is the Larmor frequency, and at low frequencies this time may be many microseconds. Any attempt to reduce the "ring-down" time also decreases the sensitivity and so Q switching is often employed. With this technique, the Q is held low whilst the transmitter is on and rapid ring-down occurs at the end of the pulse. The Q is then returned to its original value. An example of such a circuit is contained in reference (45) and a decrease of a factor of two in recovery time is obtained due to careful design. The problem with Q switching is that the transient associated with the switching causes the undamped circuit to ring anew. If this effect is small enough however, the systematic noise it introduces in the FID may be removed by a Phase Alternating Pulse Sequence (PAPS)[46] where alternate addition and subtraction into the storage device used is associated with transmitter phases of 0° and 180° respectively. The signal accumulates, the systematic noise cancels.

At very low frequencies, it is possible to retain sensitivity whilst severely limiting ring-down. The principle of the circuit used is shown in Fig. 54. The gain of the operational amplifier is sufficiently large to ensure good noise performance and a low input impedance which dampens the tuned circuit. However, care must be taken with the circuit layout and gain, or instability may occur. With a cross-coil system, crossed diodes on the amplifier input afford sufficient protection. A novel method of avoiding the problem at higher frequencies has been proposed by Lowe and colleagues.[47] Their coil is effectively a transmission line, made by deliberately introducing distributed capacitance to the coil. The characteristic impedance of the coil matches the lines used and so very rapid rise and fall times are achieved at the expense, as usual, of some sensitivity.

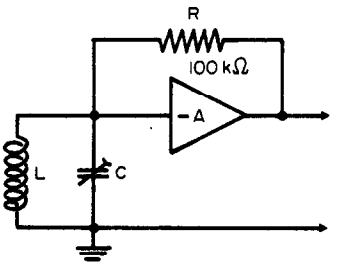

FIG. 54. Negative feedback damping.

10. PRE-AMPLIFIER DESIGN AND PROTECTION

10.1 *Protection*

Above about 150 MHz, crossed diodes lose their effectiveness as protection devices due to their inherent inductance and capacitance. Unless special care is taken with the mounting of the diodes, the inductance prevents a good short circuit being made by them when conducting. Conversely when they are not conducting, their capacitance (typically 4 pF) provides a path for high frequencies, allowing transmitter noise to reach the receiver. What is worse, impurities in the semiconductor create spurious energy levels in the band-gap. During conduction these levels are populated, but after conduction there is only a thermal relaxation mechanism and so the levels are depopulated slowly. This leads to a change in the diode capacitance of up to 20% following a radio frequency pulse, and then a non-exponential relaxation to the original value over a period of milliseconds. If the diodes' capacitance as in Fig. 20 form, at high frequencies, a major part of the noise-matching circuit in the pre-amplifier, the noise figure of the latter will be degraded immediately following the pulse and there will also be a change of phase of the signal. In severe manifestations of this effect, the pre-amplifier may oscillate after the pulse or the free induction decay may be distorted.

Above about 150 MHz it is therefore advisable to use some other form of protection. One possibility is a circulator[115]—a ferrite device having unidirectional properties. It must be remembered however that such a device must be kept well clear of the fringing field of a magnet. This is turn implies long leads to the probe and a consequent loss of sensitivity. A typical noise figure for a receiver employing a circulator is about 3 dB. PIN diodes may be used very successfully as RF switches, but a major problem is that when they have a low resistance, they are also passing a substantial direct current (40 mA) and this generates shot noise. An amplifier constructed by the author had its noise figure degraded by 4 dB when a PIN diode used as protection was passing current. A circuit is therefore needed which isolates the transmitter, yet connects the probe and pre-amplifier together when all PIN diodes are off.[48] Such a circuit is shown in Fig. 55. Point A is at a node in the standing wave pattern generated when the transmitter is on and the diodes are conducting. To see how this is so, we first note that line AE is *electrically* $\lambda/4$ long, adjustment being provided by capacitor E. There is, therefore, a short circuit of resistance about 1 Ω at point A. Now points B and D are a quarter wavelength removed from A and so the effect of lines BA and DA can be ignored, for they transform the low impedance at A to a high impedance at B and D. Power therefore flows from the transmitter to the probe in an unhindered manner via line DCB. The important point however is that there is a phase difference of 180° in the transmitted wave between

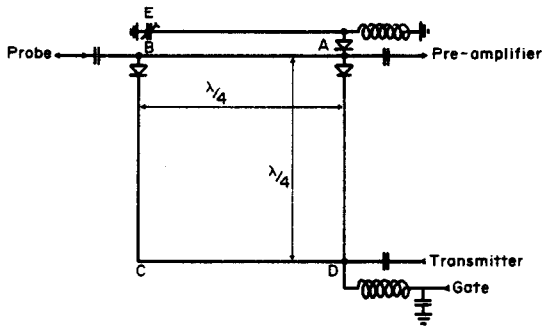

FIG. 55. A box isolator for UHF pre-amplifier protection.

points B and D. Thus the standing waves in lines BA and DA are also 180° out of phase and cancel at A. There is not only a short circuit at A, there is also a node, and so the voltage at that point is typically 60 dB less than the transmitter voltage. Similarly, the isolation of the transmitter when the diodes are off is of the same order, and there then exists a direct path from the probe to the amplifier. The manner of construction of the circuit is all important. The impedance continuity of the lines *must* be maintained at all points, and the diodes *must* form part of the lines. If this point is borne in mind, it will be found that the lines can be measured with a rule and cut to length with confidence, the capacitor at E providing the necessary adjustment. The physical length of the line AE should be a little less than $\lambda/4$. With this arrangement and a GaAs pre-amplifier, a noise figure (as measured from point B) of about 1 dB may be obtained.

10.2. *Design and Noise Measurement*

The importance of noise matching has been emphasised in Section 4.2. However, NMR poses a major problem in pre-amplifier design, for the signal source (the probe) is mainly reactive; it is resistive (50 Ω say) only at the Larmor frequency. There is always a feedback path present between the load of the transistor used in the first stage of amplification and the input circuitry, and the absence of resistive loading on the input therefore results in oscillation. To combat this effect, "neutralization"[49] of the feedback is required, and Fig. 56 shows a simple circuit for achieving this. Feedback is usually transmitted through the drain-gate capacitance of the FET in this circuit (shown by the dotted line). To neutralize it, the voltage on the drain is inverted by transformer T and passed to the gate via capacitor Z. The value of Z should of course be equal to the feedback capacitance. If the drain and gate have been shielded from one another, Z is a fraction of a picofarad for a GaAs transistor. Adjustment of Z is simple and is accomplished, at the same time as noise matching, as follows. (We refer to Fig. 20.)

As has already been mentioned, the optimum source resistance for the best noise performance is about 1 kΩ, depending on frequency. (With a GAT 1 transistor, the gate bias should also be adjusted to give about 5 mA drain current.) Assuming, as before that the value is 800 Ω, we proceed by temporarily soldering a resistance of 820 Ω across inductance M. The resistance should be 1/4 or 1/2 watt moulded carbon, for this type of resistance has good radio frequency properties. The input to the pre-amplifier is then matched to 50 Ω by adjustment of X and Y. The power to the circuit should be on for this operation and the FET should not be overloaded by the input signal (100 mV maximum). Z is correctly adjusted when variation of the tuning capacitor U has no effect upon the input matching. Of course, U is finally adjusted for maximum output from the circuit. After removing the 820 Ω resistor, we now need some method of measuring the noise figure of the pre-amplifier. Assuming that the pre-amplifier is complete, and that a spectrometer is available, the simplest method of measurement is to monitor the noise output of the spectrometer whilst changing the temperature of a 50 Ω load on the pre-amplifier input. For this purpose, it is convenient to measure the noise output with an a.c. voltmeter over a pass band of 20 Hz to 20 kHz, and to have available a 50 Ω load at room temperature and another in liquid nitrogen (77 K). The latter may be made with a moulded carbon resistor (typically 43 Ω at room temperature) soldered and shielded at the end of a co-axial cable. Let the measured RMS noise voltage at room temperature (assumed to be 20°C) be α. Let the measured RMS voltage with the 77 K resistor be β. Then the noise figure in dB is given by

$$F = -1.279 - 10\log_{10}\left(1 - \frac{\beta^2}{\alpha^2}\right)\text{dB}. \qquad (47)$$

The capacitors X and Y (Fig. 20) have already been set to the approximately correct values, but it is now a simple matter to measure the noise figure for various settings of these two. In practice, the best value is usually obtained when X is a little larger than the value required for a resistive transformation,[50] i.e. the input circuit is slightly capacitive.

In order to obtain the best performance, the gain of the first stage must be large enough to render the

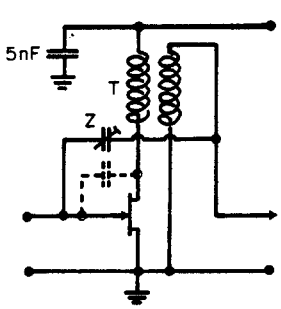

FIG. 56. Neutralization by signal inversion (see also Fig. 20).

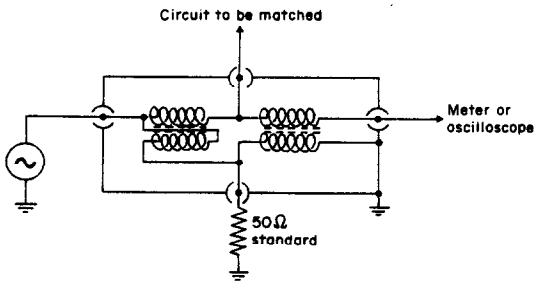

FIG. 57. A simple matching circuit. The two transformers are each three or four turns on a ferrite bead.

second stage noise negligible. The latter of course depends to some extent on the output impedance of the first stage. As this departs from the optimum value of 800 Ω, so the gain of the first stage must be increased to compensate for the worsening second stage performance. With a silicon FET, a drain load of say 2 kΩ may be needed to obtain a gain of 20 dB. This normally implies a tuned drain load with a Q of at least 20, and the bandwidth of the amplifier may be rather narrow in consequence. At low frequencies a bipolar transistor may therefore be preferred, whilst at high frequencies, a GaAs transistor will give superior performance. In general, broadband pre-amplification will sacrifice some sensitivity, and it must also be remembered that if the bandwidth of the pre-amplifier is greater than twice the Larmor frequency of interest, harmonic noise may be frequency changed in the following mixer, so degrading the total noise figure of the spectrometer.

10.3. *Matching to* 50 Ω

Much emphasis has been placed throughout the present article upon matching various circuits to 50 Ω resistance. In general, matching is best performed with the aid of a vector impedance bridge, but there is a simple and inexpensive method, utilising bifilar transformers, shown in Fig. 57. The circuit should be constructed with as much physical symmetry as possible. If this precaution is followed, a good null will be obtained up to at least 300 MHz. If possible, the null should be observed on an oscilloscope, as the presence of harmonics in the frequency source can give anomalous readings on a voltmeter.

11. DISTORTION AND RECOVERY TIME

The subject of distortion has been largely neglected in the literature, possibly because it is of no importance in CW spectroscopy, where it results merely in a slight error in line height. However, it is of great importance in Fourier Transform NMR for it can introduce baseline artefacts and even spurious spectral lines. We can distinguish two types of distortion, time dependent and time independent. The first is due to a transient overload of the receiver, for example, pulse breakthrough, whilst the second is the natural non-linearity of the electronics.

11.1. *Recovery Time Effects*

Pulse breakthrough causes ringing which is approximately described in time by the Fourier transform of the transfer function of the entire spectrometer. The duration of the ringing is mostly determined by the type of audio frequency filtering employed prior to the analogue to digital converter of a computer; the sharper the filter cut off, the longer the ringing. The accumulation of this ringing pattern along with the FID results, after Fourier transformation, in absorption and dispersion mode baselines which describe the real and imaginary parts of the transfer function respectively. The more complex the filter, the more contortions these baselines perform. A simple, and rather poor, way of eliminating this baseline distortion is to wait until the ringing has ceased before accumulating the FID. It is not generally realised, however, that this waiting time introduces, instead of baseline distortion, spectral distortion. One cannot throw away information in the FID by waiting for the receiver to "recover", and then hope to regain it by mathematical manipulation—in this case a linear phase correction across the spectrum. Accumulation must commence at the time of the RF pulse. The truncation introduced by the use of a delay Δ prior to accumulation can easily be calculated as follows. Suppose a FID is given by $e^{-t/T_2}e^{j\omega_0 t}$. It is accumulated from time Δ onwards, so let $t' = t - \Delta$. The accumulated FID is thus $(e^{-\Delta/T_2}e^{j\omega_0\Delta})(e^{-t'/T_2}e^{j\omega_0 t'})$. Now the Fourier transform of the second part of this expression is the normal Lorentzian line, but if we have several lines in the spectrum, we may observe from the first part of the expression that there is an added dependence of line height upon T_2 (viz $e^{-\Delta/T_2}$) and that there is also a phase variation with Larmor frequency (viz $e^{j\omega_0\Delta}$). For a high resolution spectrum where $T_2 \gg \Delta$, the additional T_2 dependence can be ignored; for broader lines, it cannot, and line heights are in error. The phase variation is compensated for by a linear phase correction, so that the spectrum is multiplied by a term $e^{-j\omega\Delta}$. For one particular line selected out of the many in the spectrum, let $\omega = \omega_0 - \delta\omega$. Then the phase correction applied to the spectrum about

FIG. 58. Truncation effects on two Lorentzian lines.

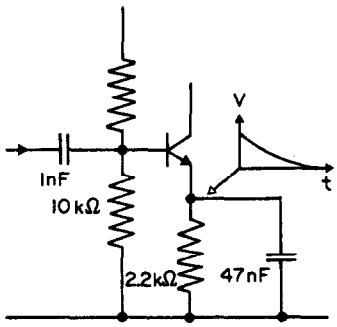

FIG. 59. A typical biassing system for small-signal RF amplifiers. It results in paralysis after gross overload.

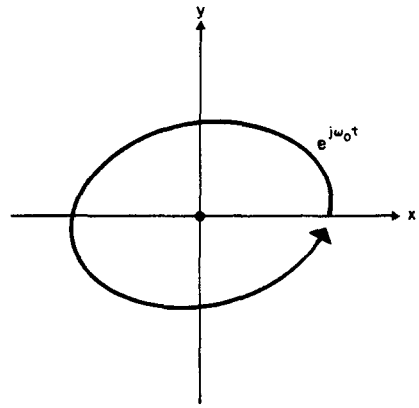

FIG. 61. Astigmatic distortion caused by amplitude and phase errors in the two receiving channels of a quadrature detection system.

that line is given by $e^{j\omega_0\Delta}e^{-j\omega\Delta} = e^{j\delta\omega\Delta}$, and this means that the wings of each spectral line have varying phase. For this effect to be negligible, $T_2 \gg \Delta$. An example of this type of truncation is shown in Fig. 58. It is often present in biological spectra in the wings of the water peak, giving rise to baseline oscillations.

Clearly, the correct way to deal with pulse breakthrough is to eliminate it by suitable gating of the receiver. The use of a Phase Alternating Pulse Sequence (PAPS)[46] then eliminates systematic noise caused by switching transients. Truncation can never be avoided totally as there is always a delay whilst the ringing of the probe ceases, and so, for very broad lines, it may be necessary to dampen that ringing (see Section 9.3). However, correct gating effects a massive improvement and certainly, for high-resolution spectra, renders truncation negligible.

Another problem which may be encountered is that the gain of the spectrometer decreases and then recovers immediately after the pulse. Apart from the diode capacitance effect mentioned earlier (Section 10.1) this can also be caused by incorrect circuit design, and results in a "dip" under each line in the spectrum. A typical biassing technique for high frequency amplification is shown in Fig. 59. Under conditions of gross a.c. overload, both capacitors become charged because the transistor acts as a diode. When the overload ceases, the transistor is biassed off and conduction slowly recommences (with accompanying gain change) over many tens of microseconds. Clearly, all time constants in the circuitry should be much than say 1 μs, apart from decoupling applications on the power lines, where, for stability's sake, it is better to go to the opposite extreme and make them very long. A time constant of 100 ms is a good value as it also reduces 50/60 Hz ripple. In this context, it should be remembered that electrolytic capacitors will not decouple radio frequencies and so capacitors in parallel are required.

Assuming that all the precautions outlined above have been taken, and that accumulation of the FID commences at the time of the RF pulse, the Fourier transform of the decay will still show a phase variation across the spectrum, and this is right and proper for these effects indicate that the filter prior to the computer is doing its job. The spectrum has been multiplied by the transfer function of the spectrometer and if this function is known, it is a simple matter for the computer to remove the effect. This tech-

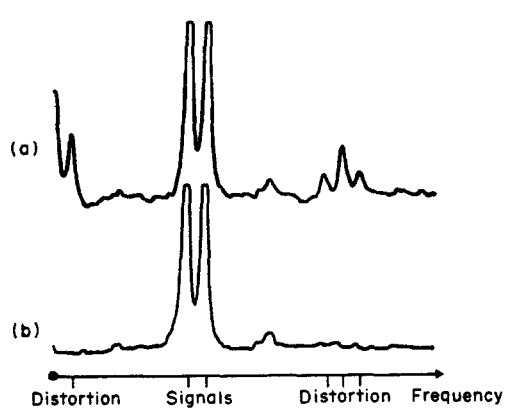

FIG. 60. Spurious signals can be generated by distortion. The effects of second-order terms are shown (a), and these may be removed (b), with the aid of a phase alternating pulse sequence.

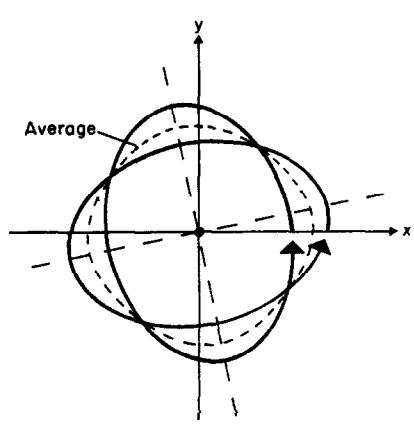

FIG. 62. Rotation of the transfer function by 90° results, upon averaging, in cancellation of astigmatism.

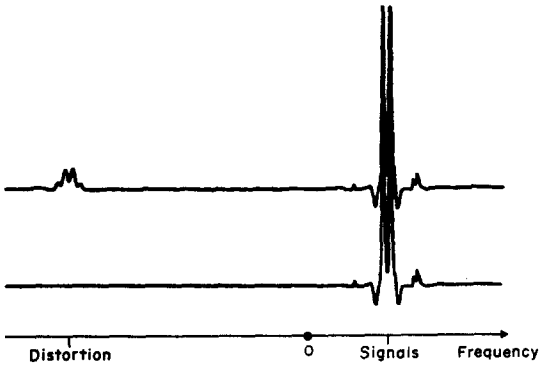

FIG. 63. Third-order distortion generates a spurious quartet from a doublet. This may be removed by the appropriate rotation of the corresponding transfer function.

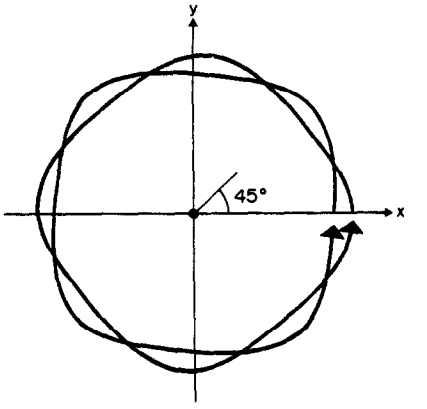

FIG. 64. The effect of third-order distortion upon the transfer function. A rotation of 45° results, upon averaging, in the cancellation of the non-linearity.

nique[51] is easily applied, but, curiously, little used. Let the transfer function of the spectrometer (i.e. the filter) be $G(\omega)$, whilst the true spectrum is $F(\omega)$. Then the spectrum obtained after Fourier transformation is $F(\omega)\,G(\omega) = H(\omega)$.

$$F(\omega) = \frac{H(\omega)G^*(\omega)}{G(\omega)G^*(\omega)} = \frac{H(\omega)G^*(\omega)}{|G(\omega)|^2} \tag{48}$$

and the computer can perform this calculation very rapidly. Alternatively, if we express $G(\omega)$ in polar coordinates, $G(\omega) = |G(\omega)|\,e^{j\Phi(\omega)}$. Equation (48) then becomes

$$F(\omega) = \frac{H(\omega)}{|G(\omega)|}\,e^{-j\Phi(\omega)} \tag{49}$$

Manufacturers are much in favour of four-pole Butterworth filters as the function $\Phi(\omega)$ (the frequency-dependent phase shift) is almost linear with frequency over the passband of these filters. $\Phi(\omega) = 180°$ at the cut off frequency (−3 dB point) and if this is placed at the Nyquist frequency of the computer, a particularly simple linear phase correction results. Of course the variation in the amplitude $|G(\omega)|$ has to be considered separately and is often ignored, leading to errors of up to 30% in amplitude in the extremities of the spectrum.

11.2. *Non-linearity*

In general, the transfer function of any electronic system is described by a power series of the form

$$V = \sum_{i=0}^{\infty} a_i(\xi)^i \tag{50}$$

Ideally, all the coefficients other than a_1 should be zero in an NMR receiver; in practice, this is not the case, and non-linearities arise in all stages of the receiver, particularly in any mixers or phase sensitive detectors and in the process of analogue-to-digital conversion. If ξ is the free induction decay of a multiline spectrum, we can see that eqn (50) rapidly becomes complicated. Let us therefore restrict ourselves to terms of third order or less, and consider only a two-line spectrum of the form

$$\xi = Ae^{-t/T_2}(\cos\omega_1 t + \cos\omega_2 t). \tag{51}$$

The first-order term is the true signal, but the second-order term is given by

$$V_2 = A^2a_2e^{-2t/T_2}\{1 + \cos(\omega_2 - \omega_1)t + \tfrac{1}{2}\cos2\omega_1 t + \cos(\omega_1 + \omega_2)t + \tfrac{1}{2}\cos2\omega_2 t\}. \tag{52}$$

If second-order distortion is present in the RF sections of the spectrometer, the frequencies generated are generally outside the passband of the instrument

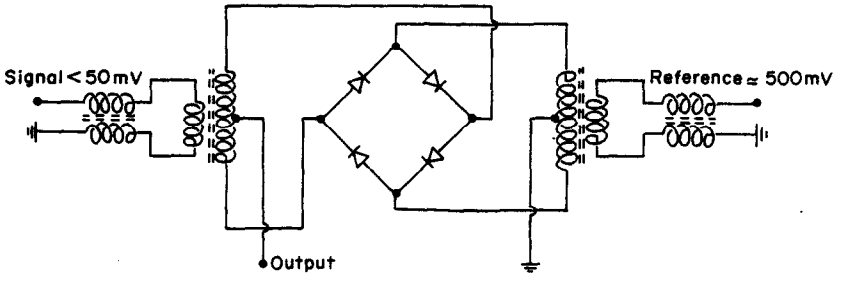

FIG. 65. A broadband RF PSD. The initial balun minimises the effect of capacitance and extends the frequency range. Diodes are types HP-5082-2970.

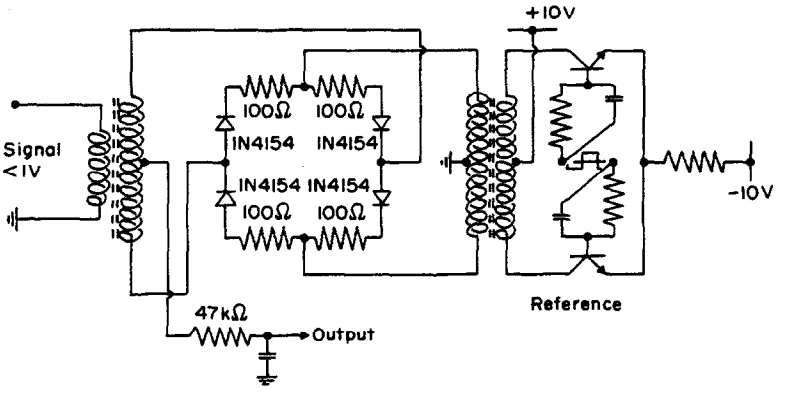

FIG. 66. A low-frequency PSD giving a distortion of less than 0.1%. The resistors and diodes are matched to 1% and the rise and fall times of the reference are better than 20 ns.

and therefore not observed, but this is not the case in the audio sections prior to the computer, and Fig. 60 shows a typical example of second-order distortion, the spurious peaks corresponding to eqn (52). This type of distortion is most commonly caused by faulty biassing on a transistor in the audio stages or by gross overload of the final phase sensitive detector. Second-order distortion can be removed by the use of a phase alternating pulse sequence and Fig. 60 shows the results of its application.

The third-order case is more complicated, and the relevant terms are;

$$V_3 = \frac{A^3 a_3}{4} e^{-3t/T_2}\{3[\cos(2\omega_1 - \omega_2)t + \cos(2\omega_2 - \omega_1)t] + [\cos 3\omega_1 t + 3\cos(2\omega_1 + \omega_2)t + 3\cos(2\omega_2 + \omega_1)t + \cos 3\omega_2 t]\}. \quad (53)$$

Let us consider first the RF sections of the instrument. The first half of the equation contains terms at about the Larmor frequency, and the non-linearity producing them is known as "intermodulation distortion". Its effect is to produce small satellites to the main lines. These may easily, in a proton spectrum, be mistaken for ^{13}C satellites. With very careful attention to design it is possible to reduce such distortion products to 0.1% or less of the main signal height, but a figure approaching 1% is easily possible if severe overload is present. If a line in a spectrum is open to question, it is best to change the RF gain of the spectrometer (or reduce the transmitter pulse width), repeat the experiment and then take the difference of the two (normalised) spectra. This will reveal clearly the distortion products.

The second half of eqn (53) corresponds to a quartet at three times the frequency of the main lines, and it is this type of distortion product which is most frequently observed, for only a slight overload of the final phase sensitive detector is needed to generate such signals. A 1% distortion is quite common, and it is not difficult to obtain 10%.

11.3. *Quadrature Detection*

Let us now expand the scope of our study of distortion by considering its effects in a system equipped with quadrature detection. In the complex plane, the transfer function of the system may be considered in optical terms, such as astigmatism, barrel distortion, etc. To understand this statement, suppose we inject into the receiver a signal at a frequency slightly removed from that of the reference. In the complex plane, the resulting Lissajous figure should be a circle. If any distortion is present, it will not be. For example, Fig. 61 shows astigmatic distortion generated by the two receiver channels being non-orthonormal. The result of this type of first-order distortion

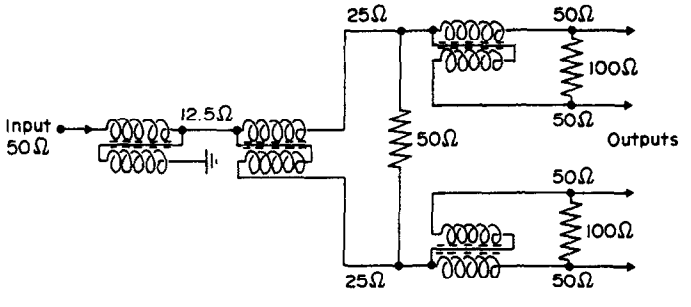

FIG. 67. A four-way splitter for use with 50 Ω systems. The outputs are isolated from one another.

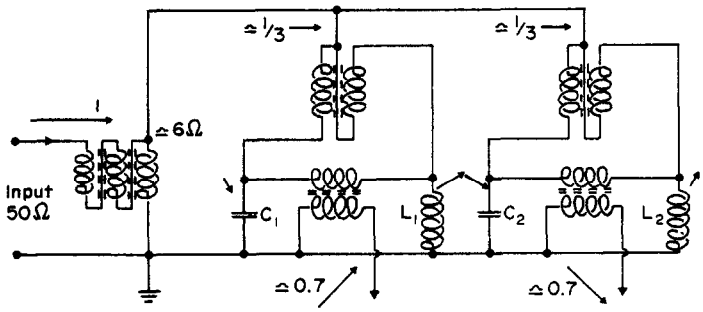

FIG. 68. A quadrature hybrid. The outputs are at phases $\pm 45°$. For a 50 Ω system $-X_{C_1} = X_{L_2} = j(\sqrt{2} - 1)50\,\Omega$; $-X_{C_2} = X_{L_1} = j(\sqrt{2} + 1)50\,\Omega$.

is the generation of a "ghost" signal[52] at the conjugate frequency; viz, a signal $e^{-t/T_2} e^{j\omega_0 t}$ has a ghost $\delta e^{-t/T_2} e^{-j\omega_0 t}$. The term δ, which is a complex quantity, is a measure of the eccentricity and orientation of the ellipse. This particular distortion may be corrected with the aid of a Cyclically Ordered Phase Sequence (CYCLOPS)[8] in the transmitter, with appropriate data routing in the computer. The purpose of the latter is to rotate the ellipse by 90°, as shown in Fig. 62. The average of the two ellipses is, to considerable accuracy, the desired circle. However, to maintain phase continuity as the computer rotates the ellipse, the transmitter must perform an opposite rotation. It has already been mentioned that subtraction into store with a corresponding transmitter phase shift of 180° eliminates second-order distortion, and this is true in the quadrature case also. Hence further rotations of the ellipse in 90° steps, with corresponding counter rotations of the transmitter, so completing a cycle, remove much distortion.

We have not yet considered fully the effects of the very common third-order distortion. Figure 63 shows a spectrum obtained, using CYCLOPS, in the presence of very bad distortion caused by overloading the final phase sensitive detectors. Note that the characteristic quartet is at three times the *conjugate* frequency. Figure 64 shows the corresponding transfer function. From this, it is quite obvious that to cancel the distortion, a rotation of 45° is required in the computer with a corresponding counter rotation in the transmitter. Figure 63 shows how effectively this technique works. If necessary, this method can be extended to higher orders. For example, a 22.5° rotation removes fifth-order products whilst CYCLOPS, having within it a 90° rotation, removes fourth-order terms. Unfortunately, unless special hardware is constructed, extra computer store is called for.

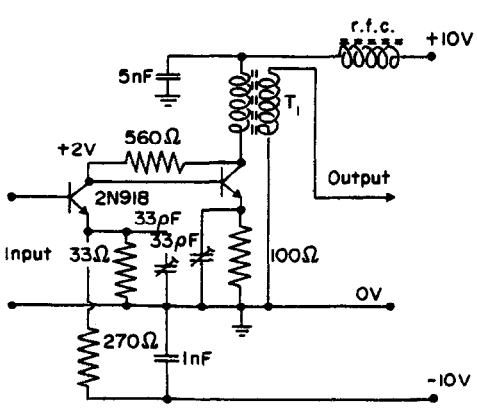

FIG. 69. A stage of wideband amplification. The input impedance is high, the output impedance is low. The gain is × 10 and the bandwidth is about 200 MHz with 2N 918 transistors.

12. CONCLUSION: USEFUL CIRCUITS

Every effort has been made in the foregoing pages to combine both theoretical and practical approaches to the problems of receiver design. No article such as the present can hope to cover every ramification of the subject and NMR will no doubt continue to issue challenges to the engineer. It is hoped, however, that the present work may serve as a useful introduction to the subject. In conclusion, a few circuits are presented which are of wide applicability. Many of them make use of broadband bifilar transformers which are wound on ferrite toroids, and an example of their use has already been given in Fig. 57. In general, low power RF circuits are best constructed on epoxy-glass printed circuit boards, the thickness of the copper being at least ten times the anticipated skin depth. In contrast to the more usual low-frequency application, the majority of copper is left on the board as a "ground plane", and connections are made by creating islands of conductor linking components. Circuits should be compact to avoid excessive inductance and capacitance, and some attempt should be made to provide a common grounding point for each stage of, say, an amplifier. The above may sound complicated; in practice, it is not, and professional standards may be achieved with a very modest outlay. Photographic processing of a mask for the board, though advisable, as it allows reduction, is not strictly necessary, for, with a careful hand, a mask may be drawn with a draftsman's pen on transparent acetate sheet. The final results are per-

fectly acceptable. Figure 65 shows a broadband PSD utilizing hot carrier diodes. The initial balun minimises the effect of capacitance and extends the frequency range, a typical value for which is 1–300 MHz. The circuit can of course also be used as a modulator or a gate with an isolation of 80 dB. A variant on this circuit for use at about 1 MHz is shown in Fig. 66. With the reference shown, a distortion of less than 0.1% is available with a signal of less than 1 V. The diodes can be any fast switching variety, but the four should be matched for reverse capacitance. Figure 67 shows a four way splitter or combiner for use with 50 Ω systems. The circuit is again broadband and the four outputs are isolated from one another. Figure 68 shows a rather more sophisticated application of broadband transformers. The input signal is split into two signals in quadrature whilst energy is conserved. Finally, Fig. 69 shows a stage of wideband amplification giving a gain of 20 dB up to about 30% of the cut-off frequency of the transistors.[53] The recovery of the circuit from overload is determined purely by the low-frequency cut-off; the small capacitors on the emitter resistors "tweak" the high frequency response.

Acknowledgements—My sincere thanks are due to Dr. R. E. Richards for his continuing support and encouragement over a period of many years and to the many members of his research group, past and present, who have stimulated my interest with proposals for NMR involving almost every branch of the science of electronics.

Funding by the Science Research Council and the Paul Instrument Fund of the Royal Society is gratefully acknowledged. Finally, I must acknowledge my debt to Mr. Peter Styles for many useful discussions and for his fund of professional expertise which has influenced considerably my approach to high frequency circuitry.

REFERENCES

1. B. Lazarew and L. Schubnikow, *Phys. Z. Sowjet* **11**, 445 (1937).
2. E. P. Day, *Phys. Rev. Lett.* **29**, 540 (1972).
3. A. Abragam, G. L. Bacchella, H. Glättli, P. Meriel, M. Pinot and J. Piesvaux, *Phys. Rev. Lett.* **31**, 776 (1973).
4. A. Abragam, *The Principles of Nuclear Magnetism*, Clarendon Press, Oxford (1961).
5. T. C. Farrar and E. D. Becker, *Pulse and Fourier Transform NMR*, Academic Press, New York and London (1971).
6. D. I. Hoult and R. E. Richards, *J. Magn. Resonance* **24**, 71 (1976).
7. H. D. W. Hill, Private Communication.
8. D. I. Hoult and R. E. Richards, *Proc. Roy. Soc. (Lond.), A* **344**, 311 (1975).
9. F. N. H. Robinson, *Noise in Electrical Circuits*, Oxford University Press, London (1962).
10. I. N. Sneddon, *Fourier Series*, Routledge and Kegan Paul, London (1961).
11. F. N. Robinson, *Noise and Fluctuations in Electronic Devices and Circuits*, Clarendon Press, Oxford (1974).
12. J. Lindmayer and C. Y. Wrigley, *Fundamentals of Semiconductor Devices*. Chapter 9, Van Nostrand, Princeton, New Jersey (1965).
13. F. E. Terman, *Electronic and Radio Engineering*, 4th edn., Chapter 4, McGraw-Hill, New York (1955).
14. I. J. Lowe and C. E. Tarr, *J. Phys. E. Ser. 2* **1**, 320 (1968).
15. S. Kan, P. Gonord, C. Duret, J. Salset and C. Vibet, *Rev. Sci. Instruments* **44**, 1725 (1973).
16. D. I. Hoult and R. E. Richards, *J. Magn. Resonance* **22**, 561 (1976).
17. Reference 13, Chapter 16.
18. D. D. Traficante, J. A. Simms and M. Mulcay, *J. Magn. Resonance* **15**, 484 (1974).
19. Radio Society of Great Britain, *The Amateur Radio Handbook*, Chapter 10, 3rd edn., RSGB, London (1964).
20. W. A. Anderson, *Rev. Sci. Instruments* **33**, 1160 (1962).
21. E. Grunwald, C. F. Jumper and S. Meiboom, *J. Amer. Chem. Soc.* **84**, 4664 (1962).
22. E. B. Baker, L. W. Burd and G. N. Root, *Rev. Sci. Instruments* **36**, 1495 (1965).
23. R. R. Ernst, *Adv. Magn. Resonance* **2**, 1 (1966).
24. R. R. Ernst and W. A. Anderson, *Rev. Sci. Instruments* **37**, 93 (1966).
25. J. Brown and E. V. D. Glazier, Telecommunications, Chapter 2, 2nd edn., Chapman and Hall, London (1974).
26. J. G. Graeme, G. E. Toby and L. P. Huelsman, *Operational Amplifiers*, Chapter 8, McGraw-Hill, New York (1971).
27. E. O. Stejskal and J. Schaefer, *J. Magn. Resonance* **14**, 160 (1974) and **15**, 173 (1974).
28. J. W. Cooper, *Computers and Chemistry* **1**, 55 (1976); *J. Magn. Resonance* **22**, 345 (1976).
29. A. G. Redfield and R. K. Gupta, *Adv. Magn. Resonance* **5**, 81 (1971).
30. F. E. Terman, *Radio Engineers' Handbook*', pp. 77–75, 1st edn., McGraw-Hill, New York (1943).
31. B. I. Bleaney and B. Bleaney, *Electricity and Magnetism*, Chapter 10, 2nd edn., Clarendon Press, Oxford (1965).
32. B. B. Austin, *Wireless Eng. Exp. Wireless* **11**, 12 (1934).
33. Reference 13, pp. 30–33.
34. J. Dadok, Private Communication.
35. C. Lafond, Third Cycle Thesis, Orsay, France.
36. H. J. Schneider and P. Dullenkopf, *Rev. Sci. Instruments* **48**, 68 (1977).
37. Reference 31, Chapter 11.
38. V. R. Cross, R. K. Hester and J. S. Waugh, *Rev. Sci. Instruments* **47**, 1486 (1976).
39. J. D. Halliday, H. D. W. Hill and R. E. Richards, *J. Phys. E. Ser. 2* **2**, 29 (1969).
40. E. R. Andrew, *Nuclear Magnetic Resonance*, pp. 56–63. The Cambridge University Press, London (1955).
41. R. R. Lembo and V. J. Kowalewski, *J. Phys. E.* **8**, 632 (1975).
42. P. C. Lauterbur, *Nature* **242**, 190 (1973).
43. D. I. Hoult, *J. Magn. Resonance* **21**, 337 (1976).
44. H. C. Torrey, *Phys. Rev.* **76**, 1059 (1949).
45. P. K. Grannell, M. J. Orchard, P. Mansfield, A. N. Garroway and D. C. Stalker, *J. Phys. E.* **6**, 1202 (1973).
46. T. Keller, US Patent 3781650, December 1973.
47. I. J. Lowe and M. Engleberg, *Rev. Sci. Instruments* **45**, 631 (1974).
48. D. I. Hoult and R. E. Richards, *J. Magn. Resonance* **22**, 561 (1976).
49. Reference 13, p. 428; reference 19, p. 50.
50. Reference 11, Chapters 11, 12 and 13.
51. Reference 29, p. 92.
52. Reference 29, p. 93.
53. E. M. Cherry and D. E. Hooper, *Proc. I.E.E.* **110**, 375 (1963).